

ARTICLE

# Platelet-activating factor (PAF) mediates NLRP3-NEK7 inflammasome induction independently of PAFR

Meng Deng<sup>1,2</sup>, Haitao Guo<sup>2,3</sup>, Jason W. Tam<sup>2,3</sup>, Brandon M. Johnson<sup>2,3</sup>, W. June Brickey<sup>2,4</sup>, James S. New<sup>5</sup>, Austin Lenox<sup>5</sup>, Hexin Shi<sup>6</sup>, Douglas T. Golenbock<sup>7</sup>, Beverly H. Koller<sup>3</sup>, Karen P. McKinnon<sup>2,4</sup>, Bruce Beutler<sup>6</sup>, and Jenny P.-Y. Ting<sup>1,2,3,4</sup>

**The role of lipids in inflammasome activation remains underappreciated. The phospholipid, platelet-activating factor (PAF), exerts multiple physiological functions by binding to a G protein-coupled seven-transmembrane receptor (PAFR). PAF is associated with a number of inflammatory disorders, yet the molecular mechanism underlying its proinflammatory function remains to be fully elucidated. We show that multiple PAF isoforms and PAF-like lipids can activate the inflammasome, resulting in IL-1 $\beta$  and IL-18 maturation. This is dependent on NLRP3, ASC, caspase-1, and NEK7, but not on NLRC4, NLRP1, NLRP6, AIM2, caspase-11, or GSDMD. Inflammasome activation by PAF also requires potassium efflux and calcium influx but not lysosomal cathepsin or mitochondrial reactive oxygen species. PAF exacerbates peritonitis partly through inflammasome activation, but PAFR is dispensable for PAF-induced inflammasome activation in vivo or in vitro. These findings reveal that PAF represents a damage-associated signal that activates the canonical inflammasome independently of PAFR and provides an explanation for the ineffectiveness of PAFR antagonist in blocking PAF-mediated inflammation in the clinic.**

## Introduction

Inflammation is a crucial host response against internal and external insults. The innate immune sentinels, pattern recognition receptors (PRRs), survey the presence of exogenous invariant microbial motifs, known as pathogen-associated molecular patterns, and endogenous danger signals released from tissue stress, known as damage-associated molecular patterns. The nucleotide-binding domain, leucine-rich-repeat-containing proteins (NLRs), represent critically evolved cytosolic PRRs as a host strategy to sense and respond to cellular insults. A subfamily of NLRs form intracellular supramolecular complexes known as the inflammasome, which activates caspase-1 and regulates the release of inflammatory cytokines IL-1 $\beta$  and IL-18, as well as the programmed inflammatory cell death called pyroptosis (Swanson et al., 2019). Several notable inflammasome-forming PRRs include NLR members NLRP1 (Martinon et al., 2002), NLRP3 (Agostini et al., 2004), NLRP6 (Elinav et al., 2011; Hara et al., 2018), NLRP7 (Khare et al., 2012), NLRP9 (Zhu et al., 2017), NLRC4 (Franchi et al., 2006; Miao et al., 2006),

and NAI1/2/5/6 (Zhao et al., 2011; Yang et al., 2013) as well as non-NLR members AIM2 (Bürckstümmer et al., 2009; Fernandes-Alnemri et al., 2009; Hornung et al., 2009), IFI16 (Kerur et al., 2011), and Pyrin (Xu et al., 2014). Most of these PRRs form inflammasomes in response to specific microbial motifs or altered self-molecules during infection.

The NLRP3 inflammasome consists of a sensor NLRP3, an adaptor apoptosis-associated speck-like protein containing a caspase recruitment domain (ASC), and an effector caspase-1 (Swanson et al., 2019). Recently, never in mitosis A-related kinase 7 (NEK7) was identified as an additional component for NLRP3 inflammasome activation (He et al., 2016; Schmid-Burgk et al., 2016; Shi et al., 2016). Upon inflammasome activation, NEK7 oligomerizes with NLRP3 to form a large complex that is essential for ASC speck formation and caspase-1 activation. The NLRP3 inflammasome is unique in that it senses a variety of stimuli, including microbial motifs during infection, danger signals during sterile inflammation, and environmental irritants

<sup>1</sup>Oral and Craniofacial Biomedicine PhD Program, University of North Carolina at Chapel Hill, Chapel Hill, NC; <sup>2</sup>Lineberger Comprehensive Cancer Center, University of North Carolina at Chapel Hill, Chapel Hill, NC; <sup>3</sup>Department of Genetics, University of North Carolina at Chapel Hill, Chapel Hill, NC; <sup>4</sup>Department of Microbiology and Immunology, University of North Carolina at Chapel Hill, Chapel Hill, NC; <sup>5</sup>Department of Microbiology, University of Alabama at Birmingham, Birmingham, AL; <sup>6</sup>Center for the Genetics of Host Defense, University of Texas Southwestern Medical Center, Dallas, TX; <sup>7</sup>Division of Infectious Diseases and Immunology, University of Massachusetts Medical School, Worcester, MA.

Correspondence to Jenny P.-Y. Ting: [jenny\\_ting@med.unc.edu](mailto:jenny_ting@med.unc.edu).

© 2019 Deng et al. This article is distributed under the terms of an Attribution-Noncommercial-Share Alike-No Mirror Sites license for the first six months after the publication date (see <http://www.rupress.org/terms/>). After six months it is available under a Creative Commons License (Attribution-Noncommercial-Share Alike 4.0 International license, as described at <https://creativecommons.org/licenses/by-nc-sa/4.0/>).

from occupational exposure. Of particular interest, modern sedentary lifestyles and increased longevity allow accumulation of danger signals, such as protein aggregates, saturated fatty acid palmitate, and crystalline particulates, which induce NLRP3-dependent sterile inflammation underlying the disease pathogenesis of multiple noncommunicable inflammatory, metabolic, and neural diseases (Wen et al., 2011; Guo et al., 2015; Mangan et al., 2018). These diverse stimuli seem to converge on three main processes involving ionic fluxes, lysosomal damage, and mitochondrial dysfunction to activate the NLRP3 inflammasome, but the precise activation mechanism remains elusive (Davis et al., 2011; Guo et al., 2015; Mangan et al., 2018; Swanson et al., 2019). Gain-of-function mutations of NLRP3 also cause a continuum of dominantly inherited autoinflammatory diseases collectively referred to as the cryopyrin-associated periodic syndromes (Hoffman et al., 2001; Yu and Leslie, 2011). In addition to the caspase-1-dependent canonical inflammasome, the caspase-11-dependent noncanonical inflammasome activated by cytosolic LPS and oxidized 1-palmitoyl-2-arachidonoyl-sn-glycerol-3-phosphatidylcholine (oxPAPC) also requires NLRP3 (Hagar et al., 2013; Kayagaki et al., 2013; Shi et al., 2014; Zanoni et al., 2016). Therefore, NLRP3 represents a critical node in regulating inflammation.

Platelet-activating factor (PAF; 1-O-alkyl-2-acetyl-sn-glycerol-3-phosphocholine) is a biologically active phospholipid mediator originally found to activate platelet aggregation (Benveniste et al., 1972). Since its discovery, extensive research has uncovered functionally diverse roles for PAF, particularly as a pathophysiological mediator in multiple inflammatory disorders such as asthma, peritonitis, anaphylaxis, and shock (Ishii and Shimizu, 2000). PAF is synthesized from and degraded to the 2-hydroxy-deacetylated derivative of PAF (lysoPAF) by PAF-acetyltransferase and PAF-acetylhydrolase, respectively (Bazan, 2003). PAF isoforms and PAF-like lipids generated through oxidation of phosphatidylcholines bind to a specific G protein-coupled seven-transmembrane PAF receptor (PAFR) that is present on most cells and triggers intracellular cascades that initiate or amplify thrombotic and inflammatory events (Yost et al., 2010). Hitherto, PAF has been recognized to function only through PAFR. However, several clinical trials using PAFR antagonists for the treatment of sepsis, asthma, and acute pancreatitis do not show clinical benefit (Spence et al., 1994; Dhainaut et al., 1998; Vincent et al., 2000; Johnson et al., 2001). This strongly suggests that additional mechanisms underlying PAF- and lysoPAF-driven inflammation may be independent of PAFR.

This report shows that both PAF and lysoPAF activate the canonical NLRP3 inflammasome in vitro and in vivo. PAF-induced IL-1 $\beta$  maturation is abrogated in macrophages from *Nlrp3*<sup>-/-</sup>, *Asc*<sup>-/-</sup>, *Nek7*<sup>-/-</sup>, and *Casp1*<sup>-/-</sup> mice, but not in cells from *Nlr4*<sup>-/-</sup>, *Nlrp1*<sup>-/-</sup>, *Nlrp6*<sup>-/-</sup>, *Aim2*<sup>-/-</sup>, *Casp11*<sup>-/-</sup>, or *Gsdmd*<sup>-/-</sup> mice. Importantly, PAFR is not required for PAF-induced NLRP3 inflammasome activation, reflecting a PAFR-independent pathway consistent with the lack of clinical efficacy of PAFR antagonists for a number of diseases. Overall, our findings reveal a new pathway for PAF and lysoPAF in inflammation that represents an unprecedented danger signaling function of these lipids and

provides new insight for understanding the pathogenesis of PAF-mediated inflammatory disorders.

## Results

### PAF induces IL-1 $\beta$ and IL-18 release

Bone marrow-derived macrophages (BMDMs) are commonly used for investigating inflammasome activation because of their efficient up-regulation of inflammasome components after priming by various stimuli, including LPS. To activate inflammasome, a second signal is required for autocleavage of procaspase-1 into active caspase-1. We tested whether C16 PAF, an isoform of PAF with a 16-carbon lipid chain, could serve as the second signal to activate inflammasome in WT BMDMs. It was selected as the prototype PAF due to its high abundance in plasma (Callea et al., 1999). Following LPS treatment, PAF robustly stimulated IL-1 $\beta$  release into the supernatant in a time-dependent manner (Fig. 1 A). In contrast, LPS or PAF alone did not induce IL-1 $\beta$  release (Fig. 1 A), confirming the two signaling hypothesis of inflammasome activation. PAF also induced IL-1 $\beta$  and IL-18 secretion in LPS-primed BMDMs in a dose-dependent fashion (Fig. 1, B–D). As expected, IL-1 $\beta$  and IL-18 release were abrogated in *Il1b*<sup>-/-</sup> and *Il18*<sup>-/-</sup> BMDMs, respectively (Fig. 1, C and D). In addition to LPS, multiple TLR ligands, including Pam3CSK4 (TLR1/2), HKLM (TLR2), FLA-ST (TLR5), FSL-1 (TLR2/6), R848 (TLR7), and ODN1826 (TLR9), but not poly(I:C) (HMW; TLR3), primed BMDMs for PAF-induced inflammasome activation (Fig. 1 E). A recent study showed that LPS can be delivered into the cell to activate caspase-11 by HMGB1 (Deng et al., 2018). However, as multiple TLR ligands primed IL-1 $\beta$  release, this rules out the possibility that PAF acts as an LPS carrier to caspase-11. Since an earlier study showed that oxPAPC activated inflammasome by binding caspase-11 intracellularly (Zanoni et al., 2016), we tested if transfected PAF could also induce IL-1 $\beta$  secretion. However, transfected PAF did not induce IL-1 $\beta$  secretion in WT BMDMs (Fig. S1).

Since PAF has multiple isoforms, we performed ex vivo testing of the activation potential of various PAF isoforms. Similar to C16 PAF, other PAF isoforms including C18L, C18H, C18:1, two PAF-like lipids, butanoyl and butenoyl, and a non-hydrolyzable carbamyl PAF all induced IL-1 $\beta$  release (Fig. 1 F). As C16 PAF is more abundant in plasma (Callea et al., 1999), we used C16 PAF in all subsequent experiments. We next addressed whether PAF could serve as the first priming signal for the inflammasome. PAF treatment followed by nigericin did not induce IL-1 $\beta$  release, which is in contrast to cells treated with LPS plus nigericin that induced IL-1 $\beta$  release (Fig. 1 G). This indicates that PAF does not serve as the priming signal. In addition, LPS-primed human macrophages and dendritic cells also secreted significant IL-1 $\beta$  in response to PAF (Fig. 1, H and I). Collectively, these data strongly suggest that PAF can serve as the second signal to induce inflammasome activation in both murine and human myeloid cells.

### PAF activates caspase-1 and ASC oligomerization

Activated caspase-1 following inflammasome assembly controls IL-1 $\beta$  maturation. Immunoblotting confirmed PAF-induced

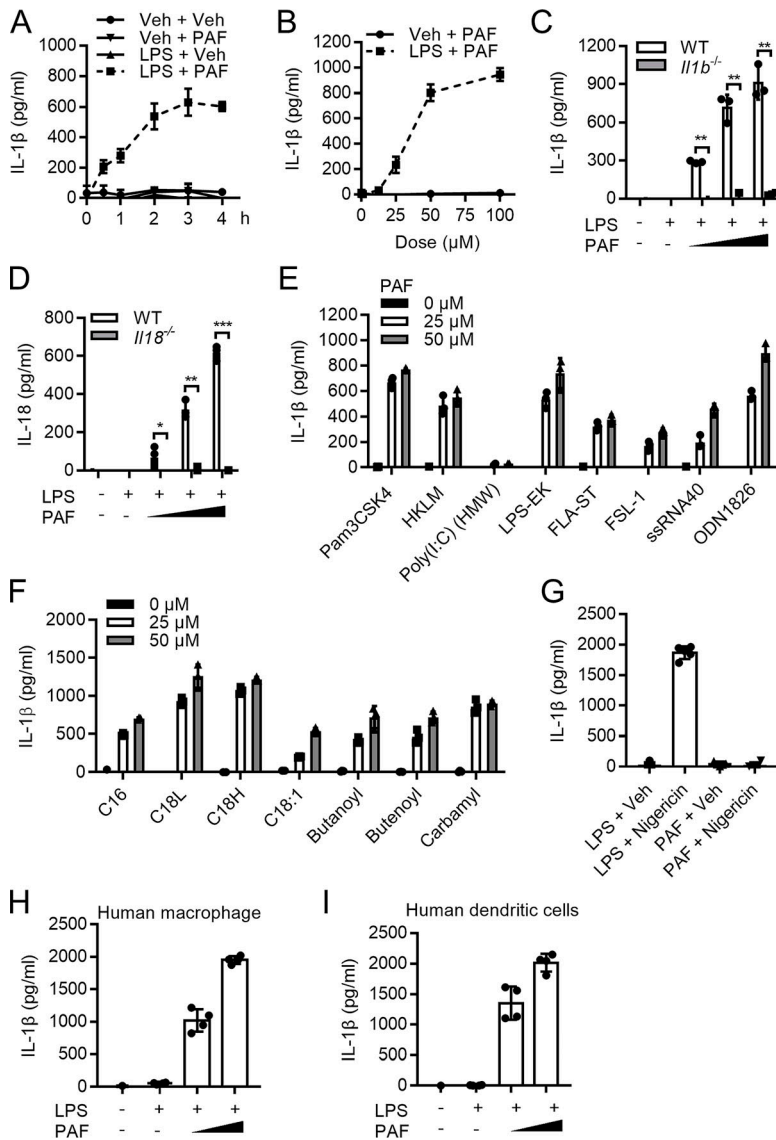


**Figure 1. PAF induces IL-1 $\beta$  and IL-18 secretion in mouse and human myeloid cells.** IL-1 $\beta$  or IL-18 ELISAs were performed in the following groups. **(A and B)** Resting or LPS-primed (300 ng/ml, 3 h) WT BMDMs stimulated with PAF (25  $\mu$ M, 3 h) for the indicated time **(A)** or with PAF at indicated concentrations for 3 h **(B)**. **(C and D)** Resting or LPS-primed (300 ng/ml, 3 h) BMDMs from WT, *Il1b*<sup>-/-</sup>, or *Il18*<sup>-/-</sup> mice stimulated with PAF (wedge, 25, 50, and 100  $\mu$ M, 3 h). **(E)** WT BMDMs primed with different TLR agonists for 3 h (1  $\mu$ g/ml Pam3CSK4 for TLR1/2, 10<sup>7</sup>/ml HKLM for TLR2, 1  $\mu$ g/ml poly(I:C) for TLR3, 1  $\mu$ g/ml LPS-EK for TLR4, 1  $\mu$ g/ml FLA-ST for TLR5, 1  $\mu$ g/ml FSL-1 for TLR2/6, 1  $\mu$ g/ml ssRNA40 for TLR7, and 200 ng/ml ODN1826 for TLR9), then stimulated with PAF (25  $\mu$ M, 3 h). **(F)** LPS-primed (300 ng/ml, 3 h) WT BMDMs stimulated with different PAF isoforms or PAF-like lipids at indicated concentrations (3 h). **(G)** WT BMDMs primed with LPS (300 ng/ml, 3 h) or PAF (25  $\mu$ M, 3 h) followed by nigericin treatment (10  $\mu$ M, 3 h). **(H and I)** Primary human macrophages **(H)** and DCs **(I)** primed with LPS (20 ng/ml, 3 h) followed by PAF (wedge, 25 and 50  $\mu$ M, 3 h) stimulation. Veh, vehicle control. Data are presented as mean  $\pm$  SD from biological replicates and are representative of three independent experiments. \*,  $P < 0.05$ ; \*\*,  $P < 0.01$ ; \*\*\*,  $P < 0.001$ , unpaired Student's *t* test.

cleavage of pro-caspase-1 to its p10 and p20 subunits and pro-IL-1 $\beta$  to its mature p17 form in both the cell lysate and culture medium (Figs. 2 A and 5 A). The pan-caspase inhibitor zVAD or caspase-1 specific inhibitor zYVAD blocked PAF-induced IL-1 $\beta$  release and maturation (Fig. 2, B and C). Therefore, PAF induces IL-1 $\beta$  maturation in a caspase-1-dependent manner.

Caspase-1 activation requires nucleation of an upstream adaptor protein ASC, another hallmark of inflammasome activation. Normally, ASC is evenly distributed in the cytoplasm, and upon inflammasome activation, ASC polymerizes and assembles into a large aggregate, known as a “speck.” The ASC-citrine transgenic mouse expresses an ASC that is citrine-labeled, thus allowing the visualization of ASC speck formation (Tzeng et al., 2016). PAF treatment following LPS priming, but not LPS alone, induced bright fluorescent ASC-citrine specks in BMDMs from these mice (Fig. 2 D). PAF treatment also induced ASC oligomerization in LPS-primed WT BMDMs (Fig. 2 E). Nigericin, a strong canonical NLRP3 inflammasome agonist, served as a positive control that induced pro-caspase-1 and pro-IL-1 $\beta$  cleavage, as well as ASC

oligomerization and speck formation, as expected (Fig. 2, A, D, and E). Therefore, in addition to caspase-1 and IL-1 $\beta$  processing, PAF induces ASC inflammasome complex formation.

**PAF activates NLRP3 inflammasome**

These data above suggest that PAF is a bona fide inflammasome activator. Next, we investigated which inflammasome effector was activated by PAF. BMDMs were generated from mice deficient in genes encoding various inflammasome components. Then, these cells were stimulated with LPS followed by PAF. Canonical inflammasomes require ASC and caspase-1 to cleave pro-IL-1 $\beta$ . A noncanonical pathway using caspase-11 has been reported to recognize cytosolic LPS and oxPAPC and thereby induce pro-IL-1 $\beta$  processing (Hagar et al., 2013; Kayagaki et al., 2013; Shi et al., 2014; Zanoni et al., 2016).

We first addressed whether PAF activated the canonical or noncanonical inflammasome pathway. PAF-induced IL-1 $\beta$  processing was abrogated in LPS-primed BMDMs from *Casp1*<sup>-/-</sup> and *Asc*<sup>-/-</sup> mice, but not from *Casp11*<sup>-/-</sup> mice (Fig. 3, A and B), indicating that PAF activates the canonical inflammasome. Next, we

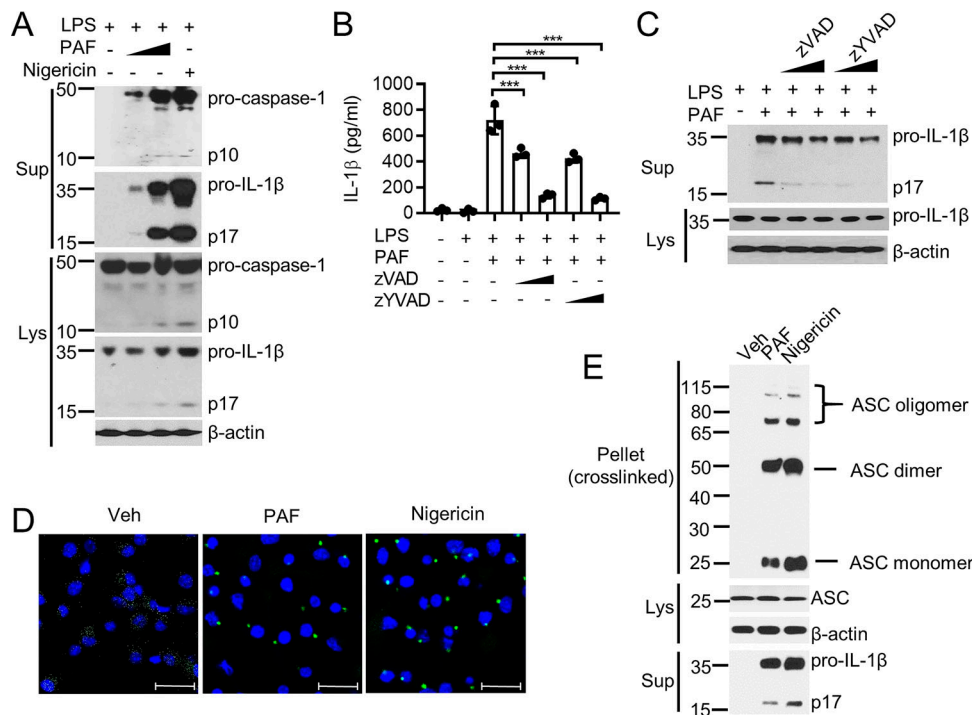


**Figure 2. PAF induces caspase-1 and IL-1 $\beta$  processing and ASC oligomerization.** (A) Immunoblotting for caspase-1 and IL-1 $\beta$  using supernatants (Sup) and cell lysates (Lys) of LPS-primed (300 ng/ml, 3 h) WT BMDMs stimulated with PAF (wedge, 25 and 50  $\mu$ M, 3 h) or nigericin (20  $\mu$ M, 3 h). (B and C) IL-1 $\beta$  ELISA (B) and immunoblotting (C) using LPS-primed (300 ng/ml, 3 h) WT BMDMs stimulated with PAF (25  $\mu$ M, 3 h) in the absence or presence of the pan-caspase inhibitor zVAD (wedge, 10 and 50  $\mu$ M) or caspase-1 inhibitor zYVAD (wedge, 10 and 50  $\mu$ M). (D) Confocal microscopy of LPS-primed (300 ng/ml, 3 h) ASC-citrine BMDMs stimulated with PAF (25  $\mu$ M, 3 h), nigericin (10  $\mu$ M, 3 h), or vehicle control (Veh). Green, ASC speck; blue, DAPI. Bars, 20  $\mu$ m. (E) Immunoblotting of ASC oligomerization using cross-linked lysates of WT BMDMs treated in the same way as in D. Data are representative of three independent experiments. Data in B are presented as mean  $\pm$  SD from biological replicates. \*\*\*,  $P < 0.001$ , one-way ANOVA. Protein marker size, kilodaltons.

tested which canonical inflammasome effector is activated by PAF. PAF-induced IL-1 $\beta$  processing and secretion were abrogated in LPS-primed BMDMs from *Nlrp3*<sup>-/-</sup> mice, but not from *Nlr4*<sup>-/-</sup>, *Aim2*<sup>-/-</sup>, *Nlrp1*<sup>-/-</sup>, or *Nlrp6*<sup>-/-</sup> mice, indicating that PAF specifically activates the canonical NLRP3 inflammasome (Fig. 3, A and C-G). Similar results were obtained with bone marrow-derived dendritic cells (BMDCs; Fig. 3, H-K). As controls for the specificity and integrity of cells derived from gene deletion strains, we showed that inflammasome activation by nigericin was dependent on NLRP3, ASC, and caspase-1; cytosolic poly(dA:dT) was dependent on AIM2, ASC, and caspase-1; cytosolic flagellin was dependent on NLRC4 and caspase-1 and partially dependent on ASC; and cytosolic LPS was dependent on caspase-1, ASC, caspase-11, and NLRP3 (Fig. 3 A). Taken together, these results point to PAF's role in activating the canonical NLRP3 inflammasome.

**PAF-activated inflammasome requires NEK7 and is inhibited by an NLRP3 inhibitor, MCC950**

NEK7 has been newly identified as an essential interaction partner of the NLRP3 inflammasome that is required for its function (He et al., 2016; Schmid-Burgk et al., 2016; Shi et al., 2016). NEK7 is specifically required for NLRP3, but not NLRC4 or AIM2, inflammasome activation, nor for TLR priming. Importantly, *Nek7* deficiency abolished IL-1 $\beta$  processing and secretion induced by PAF (Fig. 4, A and B). It also reduced inflammasome

activation by NLRP3-dependent activators, including nigericin, ATP, silica, and cytosolic LPS, but not by the AIM2 or NAIP/NLRC4-dependent activators poly(dA:dT) and flagellin, respectively (Fig. 4, A and B). Thus, NEK7, a specific NLRP3 inflammasome component, is required for PAF-induced inflammasome activation. By contrast, *Nek7* deficiency does not impact LPS priming, as WT and *Nek7*<sup>-/-</sup> BMDMs produced the same amount of TNF in response to LPS (Fig. 4 C).

MCC950 is known as a chemical inhibitor that specifically inhibits NLRP3 inflammasome activation, but not the priming phase (Coll et al., 2015, 2019). Consistently, MCC950 did not alter LPS priming, as increasing doses of MCC950 did not change NLRP3 or pro-IL-1 $\beta$  protein expression or TNF secretion induced by LPS (Fig. 4, D and E). However, MCC950 blocked IL-1 $\beta$  processing and secretion induced by PAF, nigericin, and cytosolic LPS, but not by transfected poly(dA:dT) or flagellin (Fig. 4, F and G). Collectively, these genetic and pharmacological data indicate that PAF specifically activates the canonical NLRP3 inflammasome.

**PAF induces gasdermin-D (GSDMD) cleavage, but induced IL-1 $\beta$  secretion is independent of GSDMD**

Inflammasome activation leads to caspase-1/4/5/11 cleavage of GSDMD, which drives lytic cell death (He et al., 2015; Kayagaki et al., 2015; Shi et al., 2015). Treating LPS-primed BMDMs revealed that PAF induced procaspase-1 cleavage into a p20

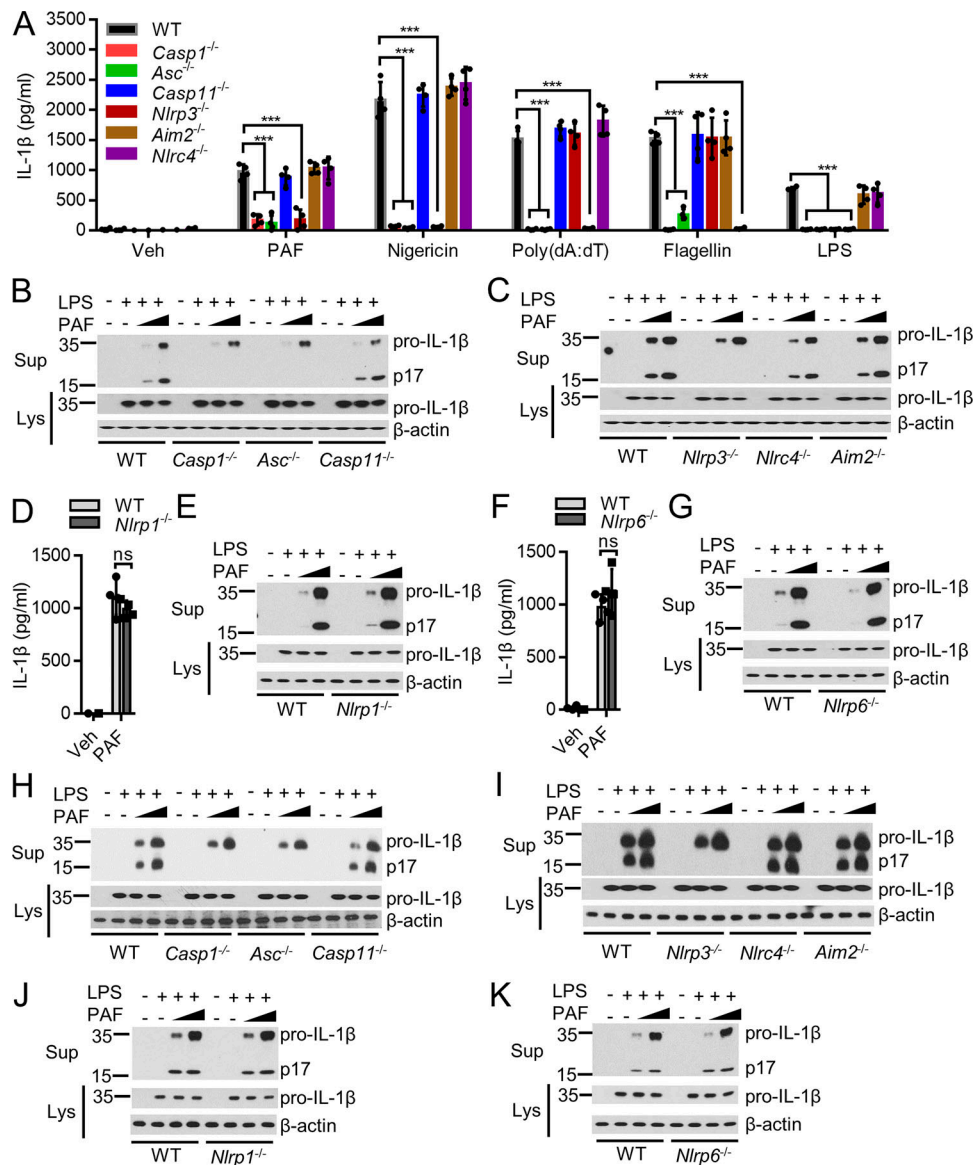


**Figure 3. PAF activates the canonical NLRP3 inflammasome. (A)** IL-1 $\beta$  ELISA using supernatants from LPS-primed (300 ng/ml, 3 h) BMDMs of indicated genotype stimulated with PAF (25  $\mu$ M), nigericin (10  $\mu$ M), transfected poly(dA:dT) (2 ng/ $\mu$ l), transfected flagellin (1 ng/ $\mu$ l), transfected LPS (1 ng/ $\mu$ l), or vehicle control (Veh) for 3 h. **(B and C)** IL-1 $\beta$  immunoblotting using supernatants (Sup) and cell lysates (Lys) from resting or LPS-primed (300 ng/ml, 3 h) BMDMs of indicated genotypes stimulated with PAF (wedge, 25 and 50  $\mu$ M) or Veh. **(D and E)** IL-1 $\beta$  ELISA (D) and immunoblotting (E) using Sup or Lys from resting or LPS-primed (300 ng/ml, 3 h) BMDMs of indicated genotypes stimulated with PAF (wedge, 25 and 50  $\mu$ M) or Veh. **(F and G)** IL-1 $\beta$  ELISA (F) and immunoblotting (G) using resting or LPS-primed Sup or Lys of BMDMs of indicated genotypes stimulated with PAF (wedge, 25 and 50  $\mu$ M) or Veh. **(H–K)** IL-1 $\beta$  immunoblotting using Sup or Lys from resting or LPS-primed (300 ng/ml, 3 h) BMDMs of indicated genotypes stimulated with PAF (wedge, 25 and 50  $\mu$ M). Data are representative of three independent experiments. Data in A, D, and F are presented as mean  $\pm$  SD from biological replicates. \*\*\*,  $P < 0.001$ . ns, not significant. One-way ANOVA (A), unpaired Student's  $t$  test (D and F). Protein marker size, kilodaltons.

subunit, and additionally induced GSDMD cleavage into the p30 subunit in both cell lysates and cell culture medium (Fig. 5 A). As a positive control, nigericin also induced GSDMD cleavage into the p30 subunit (Fig. 5 B). Recent studies showed that IL-1 $\beta$  secretion downstream of inflammasome activation can be either dependent or independent of GSDMD (Schneider et al., 2017; Evavold et al., 2018). LPS followed by PAF treatment induced comparable IL-1 $\beta$  processing and secretion in *Gsdmd*<sup>-/-</sup> cells and control cells, indicating that PAF-induced IL-1 $\beta$  secretion is independent of GSDMD (Fig. 5, C and D). Similarly, silica-induced

IL-1 $\beta$  secretion is also independent of GSDMD, whereas ATP-induced IL-1 $\beta$  secretion is dependent on GSDMD (Fig. 5 C).

Although certain NLRP3 inflammasome activators, such as ATP, induce cell death downstream of NLRP3 inflammasome activation, other activators such as lysosomal rupturing reagents and cytosolic LPS induce cell death independently of the NLRP3 inflammasome machinery (Coll et al., 2015). We tested if PAF-induced cell death is dependent on the NLRP3 inflammasome. In LPS-primed BMDMs, PAF-induced cell death was only modestly dependent on NLRP3, ASC, caspase-1, and GSDMD, with

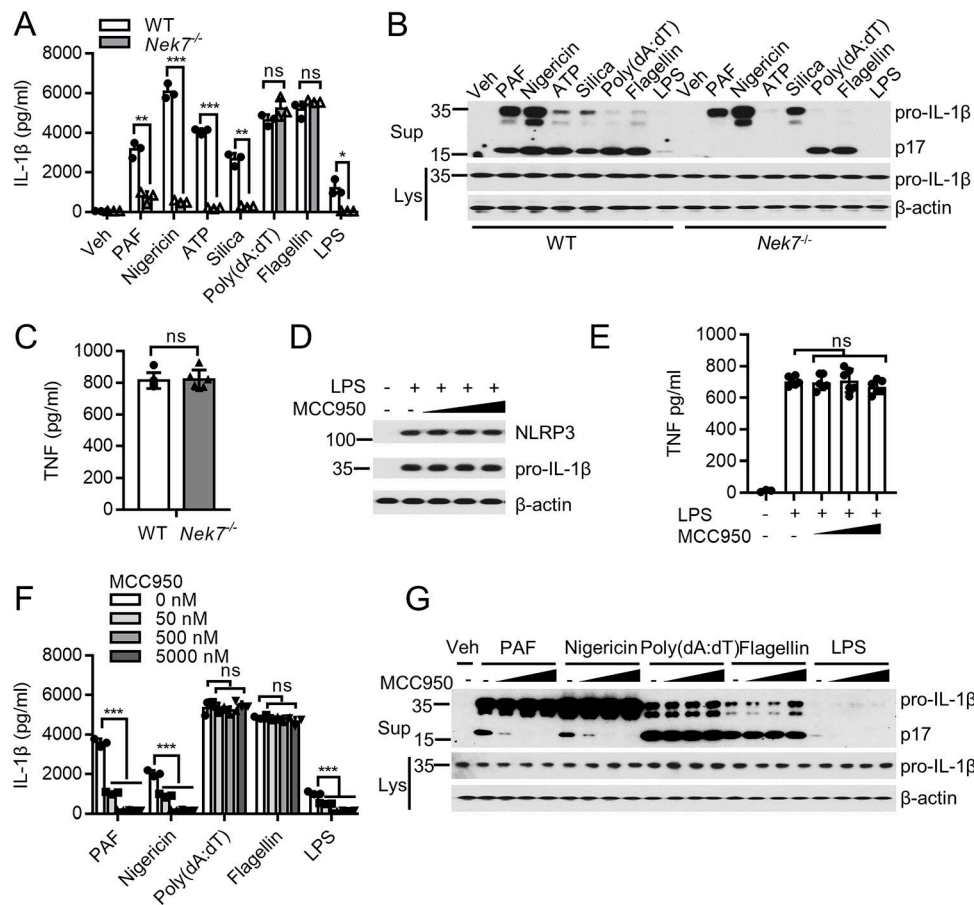


**Figure 4. PAF-activated inflammasome requires NEK7 and is inhibited by an NLRP3 inhibitor, MCC950.** (A and B) IL-1 $\beta$  ELISA (A) and immunoblotting (B) using supernatant (Sup) and cell lysate (Lys) of LPS-primed (300 ng/ml, 3 h) WT or *Nek7*<sup>-/-</sup> BMDMs stimulated with PAF (25  $\mu$ M), nigericin (10  $\mu$ M), ATP (5 mM), silica (300  $\mu$ g/ml), transfected poly(dA:dT) (2 ng/ $\mu$ l), transfected flagellin (1 ng/ $\mu$ l), transfected LPS (1 ng/ $\mu$ l), or vehicle control (Veh) for 3 h. (C) TNF ELISA using supernatants of LPS-treated (300 ng/ml, 3 h) BMDMs. (D and E) NLRP3 and IL-1 $\beta$  immunoblotting using cell lysates (D) and TNF ELISA using supernatants from resting or LPS-primed (300 ng/ml, 3 h) WT BMDMs (E) in the presence of increasing doses of MCC950 (wedge, 0, 50, 500, and 5,000 nM). (F and G) IL-1 $\beta$  ELISA (F) and immunoblotting (G) of LPS-primed (300 ng/ml, 3 h) WT BMDMs stimulated with PAF (25  $\mu$ M), nigericin (5  $\mu$ M), transfected poly(dA:dT) (2 ng/ $\mu$ l), transfected flagellin (1 ng/ $\mu$ l), transfected LPS (1 ng/ $\mu$ l), or vehicle control (Veh) in the absence or presence of MCC950 at the concentrations shown in F. Data are representative of three independent experiments. Data in A, C, E, and F are presented as mean  $\pm$  SD from biological replicates. \*,  $P < 0.05$ ; \*\*,  $P < 0.01$ ; \*\*\*,  $P < 0.001$ . ns, not significant. Unpaired Student's *t* test (A and C); one-way ANOVA (E and F). Protein marker size, kilodaltons.

significance attained depending on the time after PAF treatment (Fig. S2, A–D). The NLRP3 inhibitor, MCC950, potently inhibited IL-1 $\beta$  secretion induced by PAF, ATP, and silica (Fig. S2 E). However, MCC950 only moderately inhibited cell death induced by PAF (Fig. S2 F). As controls, MCC950 potently inhibited cell death induced by ATP, but not by silica (Fig. S2 F). Ethidium bromide (EB) is known to be excluded from the intact cell. Treating LPS-primed BMDMs with PAF, nigericin, or ATP-induced cellular permeabilization to EB (Fig. S2 G). However, while cell permeabilization caused by nigericin was dependent on NLRP3, that caused by PAF and ATP was independent of NLRP3 (Fig. S2 H). Therefore, like ATP, PAF increases cell membrane permeabilization in an NLRP3-independent manner.

#### PAFR is not involved in inflammasome activation

PAF is recognized by a unique G protein-coupled receptor (GPCR), PAFR. To assess the involvement of PAFR in inflammasome activation, we found that PAFR antagonists,

Ginkgolide B and WEB2086, did not block IL-1 $\beta$  release induced by PAF (Fig. 6 A). Pharmacologic inhibitors can have unintended targets; thus we next resorted to a genetic approach. We first explored whether inflammasome activation requires PAFR. Priming WT and *Pafr*<sup>-/-</sup> BMDMs or BMDCs with LPS triggered comparable up-regulation of NLRP3 and pro-IL-1 $\beta$  protein (Fig. 6, B and C) as well as TNF cytokine (Fig. 6, D and E), indicating that PAFR is not involved in priming. Additionally, PAF induced similar levels of IL-1 $\beta$  processing and secretion in LPS-primed WT and *Pafr*<sup>-/-</sup> BMDMs (Fig. 6, F and H) and BMDCs (Fig. 6, G and I). We also tested whether other inflammasome agonists require PAFR. IL-1 $\beta$  levels were unchanged in *Pafr*<sup>-/-</sup> compared with WT BMDMs (Fig. 6 H) and BMDCs (Fig. 6 I) upon inflammasome activation by nigericin, ATP, silica, alum, cytosolic poly(dA:dT), flagellin, and LPS. LysoPAF is generally perceived as an inactive form of PAF since it is not a PAFR agonist (Dyer et al., 2010). Consistently, C16, C18, and C18:1 lysoPAF induced IL-1 $\beta$  processing in an NLRP3-dependent manner

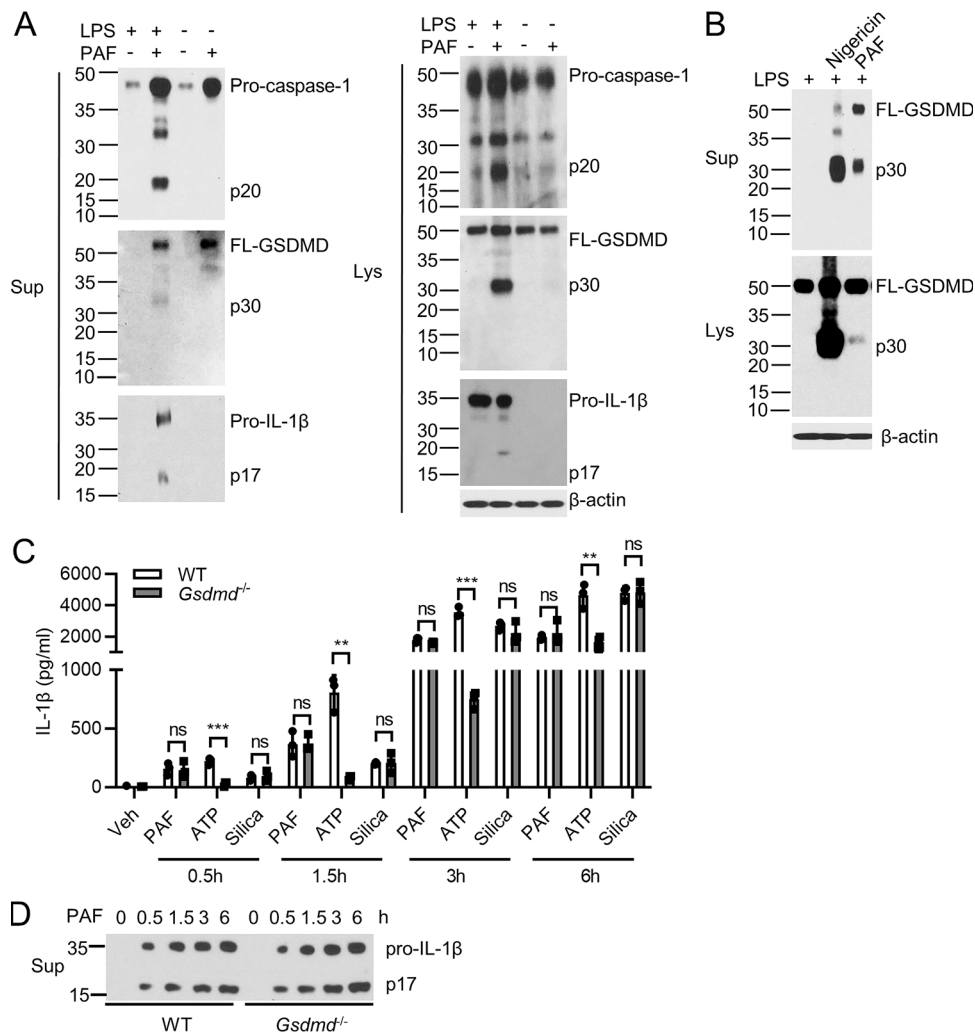


**Figure 5. GSDMD is not required for IL-1 $\beta$  secretion induced by PAF.** (A) Immunoblot of supernatants (Sup) and cell lysates (Lys) from resting or LPS-primed (300 ng/ml, 3 h) WT BMDMs stimulated with or without PAF (25  $\mu$ M, 3 h). (B) Immunoblot of Sup or Lys from LPS-primed (300 ng/ml, 3 h) WT BMDMs stimulated with nigericin (10  $\mu$ M, 3 h) or PAF (25  $\mu$ M, 3 h). (C) IL-1 $\beta$  ELISA using supernatants from LPS-primed (300 ng/ml, 3 h) WT or *Gsdmd*<sup>-/-</sup> BMDMs stimulated with PAF (25  $\mu$ M), ATP (10 mM), or silica (300  $\mu$ g/ml) for the indicated time. (D) Immunoblot of supernatants from LPS-primed (300 ng/ml, 3 h) WT or *Gsdmd*<sup>-/-</sup> BMDMs stimulated with PAF (25  $\mu$ M) for indicated time. Data are representative of three independent experiments. Data in C are presented as mean  $\pm$  SD from biological replicates. \*\*,  $P < 0.01$ ; \*\*\*,  $P < 0.001$ . ns, not significant. Unpaired Student's *t* test (C). FL, full-length. Protein marker size, kilodaltons.

(Fig. 6 J). Therefore, multiple lines of evidence are provided that PAF activates the inflammasome independently of PAFR.

**Inflammasome activation requires calcium and potassium flux, but not ROS or cathepsin**

The precise mechanism of NLRP3 inflammasome activation remains elusive. However, several mechanisms, including mitochondrial ROS production, cathepsin release upon lysosome rupture, potassium efflux, and calcium influx, have been proposed to be critical for NLRP3 inflammasome activation (Davis et al., 2011; Guo et al., 2015; Mangan et al., 2018; Swanson et al., 2019).

Calcium influx from the ER or extracellular space into the cytosol has been shown to activate the NLRP3 inflammasome (Lee et al., 2012; Rossol et al., 2012). Phospholipase C (PLC) hydrolyses phosphatidylinositol-4,5-bisphosphate into inositol

trisphosphate (InsP<sub>3</sub>), and InsP<sub>3</sub> binding to InsP<sub>3</sub> receptors (InsP<sub>3</sub>R) causes Ca<sup>2+</sup> release from the ER (Lee et al., 2012). We investigated the role of calcium influx by targeting the PLC signaling pathway. *m*-3M3FBS, a direct activator of PLC, induced IL-1 $\beta$  processing, confirming the role of PLC-mediated Ca<sup>2+</sup> signals in inflammasome activation (Fig. S3, A and B). The PLC inhibitor U73122, InsP<sub>3</sub>R inhibitor 2-aminoethoxydiphenyl borate (2-APB), and calcium chelator 1,2-bis(*o*-aminophenoxy) ethane-*N,N,N',N'*-tetraacetic acid (BAPTA) all blocked PAF-induced IL-1 $\beta$  processing and secretion (Fig. 7, A and B; and Fig. S3, C and D). As controls, U73122, 2-APB, and BAPTA did not block AIM2 or NLRC4 inflammasome activation by poly(dA:dT) or flagellin, respectively (Fig. S3, C and D). In addition, Ca<sup>2+</sup>-free medium also reduced PAF-induced IL-1 $\beta$  processing (Fig. 7 C).

Cytosolic potassium efflux has been proposed to play a central role in NLRP3 inflammasome activation (Muñoz-Planillo

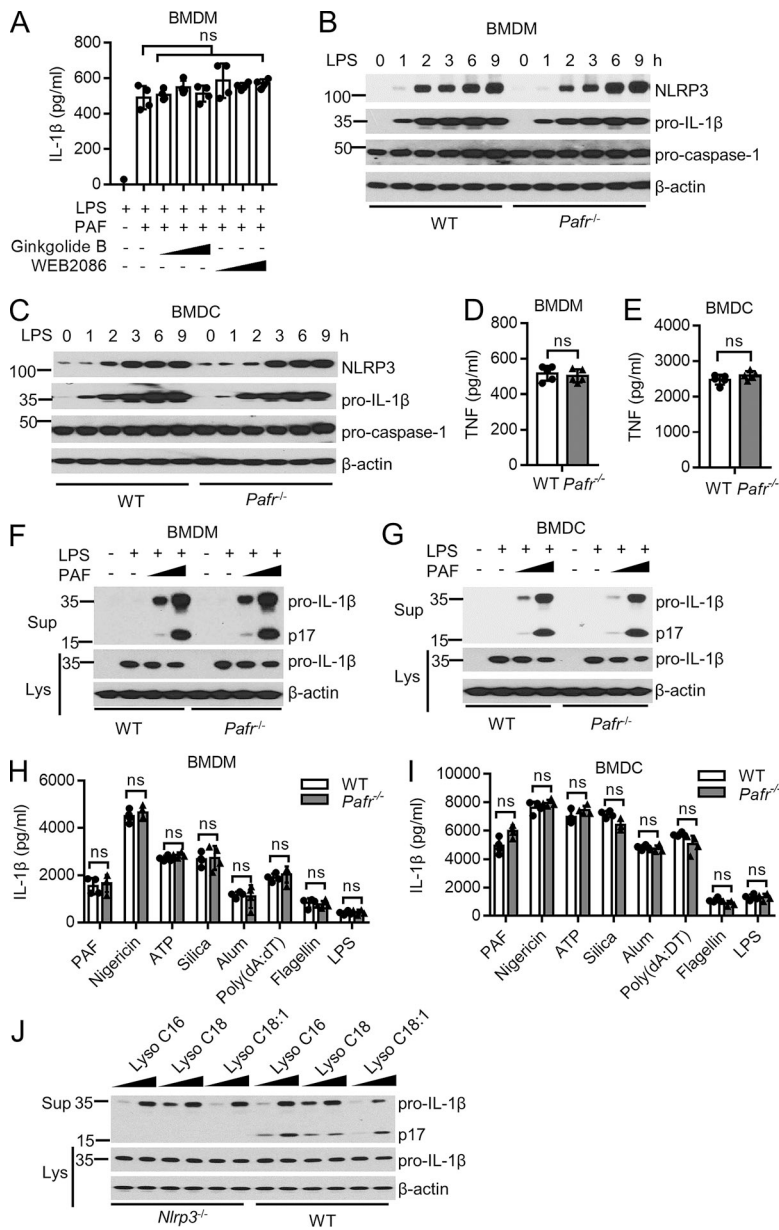


**Figure 6. PAF activation of the inflammasome is independent of PAFR.** (A) IL-1 $\beta$  ELISA using supernatants from LPS-primed (300 ng/ml, 3 h) WT BMDMs stimulated with 25  $\mu$ M PAF in the absence or presence of PAFR antagonist Ginkgolide B (wedge, 10, 50, and 100  $\mu$ M) or WEB2086 (wedge, 10, 50, and 100  $\mu$ M) for 3 h. (B and C) Immunoblot of cell lysates from WT and *Pafr*<sup>-/-</sup> BMDMs (B) or BMDCs (C) treated with LPS (300 ng/ml) for the indicated time. (D and E) TNF ELISA using supernatants from LPS-primed (300 ng/ml, 3 h) WT and *Pafr*<sup>-/-</sup> BMDMs (D) or BMDCs (E). (F and G) Immunoblot using supernatants (Sup) and cell lysates (Lys) from resting or LPS-primed (300 ng/ml, 3 h) WT and *Pafr*<sup>-/-</sup> BMDMs (F) or BMDCs (G) stimulated with PAF (wedge, 25 and 50  $\mu$ M). (H and I) IL-1 $\beta$  ELISA using supernatants from LPS primed WT or *Pafr*<sup>-/-</sup> BMDMs (H) or BMDCs (I) stimulated with PAF (25  $\mu$ M), nigericin (10  $\mu$ M), ATP (5 mM), silica (300  $\mu$ g/ml), alum (300  $\mu$ g/ml), transfected poly(dA:dT) (2 ng/ $\mu$ l), transfected flagellin (1 ng/ $\mu$ l), or transfected LPS (1 ng/ $\mu$ l) for 3 h. (J) Immunoblot of supernatants or cell lysates from LPS-primed (300 ng/ml, 3 h) WT and *Nlrp3*<sup>-/-</sup> BMDMs stimulated with the indicated lysoPAF isoforms (wedge, 25 and 50  $\mu$ M). Data are representative of three independent experiments. Data in A, D, E, H, and I are presented as mean  $\pm$  SD from biological replicates. ns, not significant. One-way ANOVA (A); unpaired Student's *t* test (D, E, H, and I). Protein marker size, kilodaltons.

et al., 2013). Increasing the extracellular K<sup>+</sup> also abolished PAF-induced IL-1 $\beta$  processing and secretion, but did not inhibit AIM2 or NLRC4 inflammasome activation by poly(dA:dT) or flagellin (Figs. 7 D and S3 E).

In contrast, the ROS scavengers *N*-acetyl-L-cysteine (NAC) and (2-(2,2,6,6-tetramethylpiperidin-1-oxyl-4-ylamino)-2-oxoethyl) triphenylphosphonium chloride (Mitotempo), NADPH oxidase inhibitor (2R,4R)-4-aminopyrrolidine-2,4-dicarboxylic acid (APDC), and diphenyleneiodonium (DPI) did not inhibit IL-1 $\beta$  processing or secretion induced by PAF (Figs. 7 E and S3 F). Imiquimod is known to activate the NLRP3 inflammasome via a burst of ROS (Groß et al., 2016). Our results show that several ROS inhibitors including NAC, Mitotempo, APDC, and DPI readily inhibited imiquimod-induced IL-1 $\beta$  secretion, but not PAF-induced IL-1 $\beta$  secretion (Fig. S3 F). Also, the cathepsin B inhibitor CA-074-Me reduced silica-induced, but not PAF-induced, IL-1 $\beta$  processing and secretion (Figs. 7 F and

S3 G). Taken together, these data suggest that PAF activation of the NLRP3 inflammasome requires Ca<sup>2+</sup> and K<sup>+</sup> flux but is independent of ROS and cathepsin B.

ATP and uric acid released during cell damage can activate the NLRP3 inflammasome (Shi et al., 2003; Mariathasan et al., 2006; Martinon et al., 2006; Piccini et al., 2008). To assess if PAF activates the inflammasome by triggering the release of ATP, we used A-740003 and A-804598, antagonists of the ATP-sensing P2X<sub>7</sub> receptor, as well as apyrase, which degrades ATP. None of these treatments impaired PAF-induced IL-1 $\beta$  processing and secretion, while all impaired ATP-induced inflammasome activation (Figs. 7 G and S4 A). Consistent with the findings using pharmacologic inhibitors, PAF induced similar levels of IL-1 $\beta$  processing and secretion in WT and *P2x7r*<sup>-/-</sup> BMDMs, whereas ATP-induced IL-1 $\beta$  processing and secretion were completely abolished (Figs. 7 H and S4 B). In addition, uricase, which degrades monosodium urate (MSU) crystals, reduced



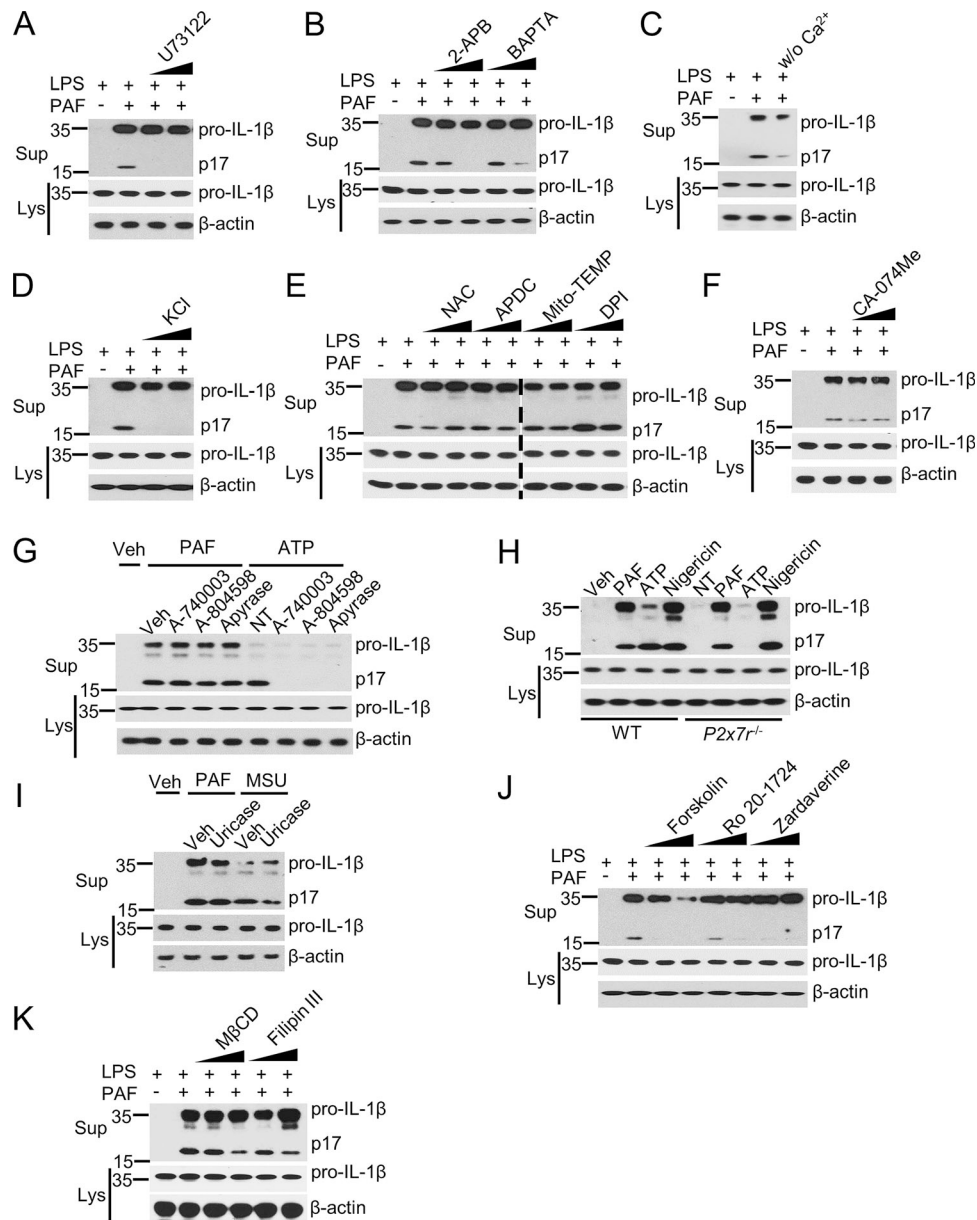


**Figure 7. PAF activation of inflammasome requires calcium, potassium flux, reduced cAMP, and intact lipid rafts, but not ROS, cathepsin, ATP, or uric acid signaling. (A–G and I–K)** IL-1 $\beta$  immunoblotting using supernatants (Sup) and lysates (Lys) from LPS-primed (300 ng/ml, 3 h) WT BMDMs stimulated with PAF (25  $\mu$ M, 3 h) in the absence or presence of indicated inhibitors or enzymes (A, B, D–G, and I–K) or cultured in Ca<sup>2+</sup>-free medium (C). Concentrations used are as follows: U73122 (2 and 10  $\mu$ M), 2-APB (20 and 100  $\mu$ M), BAPTA-AM (10 and 20  $\mu$ M), KCl (25 and 50 mM), NAC (5 and 25 mM), APDC (10 and 50  $\mu$ M), Mitotempo (100 and 500  $\mu$ M), DPI (5 and 25  $\mu$ M), CA-074-ME (10 and 20  $\mu$ M), A-804598 (100  $\mu$ M), A-740003 (100  $\mu$ M), apyrase (1 U/ml), uricase (1 U/ml), forskolin (25 and 100  $\mu$ M), ro-20-1724 (100 and 250  $\mu$ M), zardaverine (100 and 250  $\mu$ M), M $\beta$ CD (5 and 15 mM), Filipin III (2.5 and 12.5  $\mu$ g/ml). ATP (5 mM) in G. **(H)** IL-1 $\beta$  immunoblotting using LPS-primed (300 ng/ml, 3 h) WT and *P2x7*<sup>-/-</sup> BMDMs stimulated with PAF (25  $\mu$ M), ATP (5 mM), or nigericin (10  $\mu$ M) for 3 h. Veh, vehicle control. The image in E is assembled from two sections of the same blot, and the break between these two sections is indicated by a dashed line. Data are representative of three independent experiments. w/o, without. Protein marker size, kilodaltons.

MSU- but not PAF-induced IL-1 $\beta$  secretion (Figs. 7 I and S4, C and D). Therefore, PAF-induced inflammasome activation is independent of ATP and uric acid signaling.

Recently, it was shown that NOX4-dependent fatty acid oxidation promotes NLRP3 inflammasome activation (Moon et al., 2016). VAS2870, a specific inhibitor for NOX4, inhibited IL-1 $\beta$  secretion induced by PAF, nigericin and silica in BMDMs (Fig. S4 E). These results suggest that PAF-activated NLRP3 inflammasome might depend on NOX4-mediated fatty acid oxidation.

GPCR signaling can regulate NLRP3 inflammasome activity. Dopamine, bile acid, and prostaglandin E2 bind to their cognate GPCRs and stimulate adenylyl cyclase (ADCY) to synthesize cAMP, which then activates PKA to suppress NLRP3 activation (Yan et al., 2015; Guo et al., 2016; Mortimer et al., 2016). Increased cAMP synthesis by the ADCY activator, forskolin, or decreased cAMP degradation by the phosphodiesterase inhibitors, Ro 20-1724 and zardaverine, suppressed IL-1 $\beta$  processing and secretion induced by PAF but not by poly(dA:dT) or

flagellin stimulation (Figs. 7 J and S4 F). Although our earlier data suggest that PAFR is not involved in inflammasome activation by PAF in culture, other GPCRs, such as the calcium-sensing receptor, are known to activate the NLRP3 inflammasome through induction of  $\text{Ca}^{2+}$  flux and reduction of intracellular cAMP (Lee et al., 2012; Rossol et al., 2012). To explore if there are potential unknown GPCRs that mediate the effect of PAF, we tested two lipid raft inhibitors, methyl- $\beta$ -cyclodextrin (M $\beta$ CD) and filipin III, as lipid raft formation is crucial for GPCR signaling (Van Anthony et al., 2016). These inhibitors alone did not induce IL-1 $\beta$  release (Fig. S4 G), but rather moderately inhibited IL-1 $\beta$  processing and secretion induced by PAF but not by poly(dA:dT) or flagellin (Figs. 7 K and S4, H and I). These data suggest that PAF-induced inflammasome activation is regulated by the cAMP-PKA axis and potentially by other receptors in lipid rafts.

### PAF induces NLRP3-dependent peritonitis in vivo

The in vitro results delineated a proinflammatory activity of the PAF family of lipids in activating the NLRP3 inflammasome that appeared to be independent of PAFR. To confirm such a role in vivo, we used an established inflammatory peritonitis model, since PAF is elevated in peritonitis in humans (Montrucchio et al., 1989). Mice were primed with or without i.p. injection of LPS for 3 h, followed by challenge with C-16 lysoPAF alone, C-16 lysoPAF combined with the NLRP3 inhibitor MCC950, or vehicle control. Serum cytokines and peritoneal neutrophil influx were measured 6 h after challenge (Fig. 8 A). Mice that received vehicle, LPS, or C-16 lysoPAF alone displayed undetectable or low levels of serum IL-1 $\beta$ , IL-18, and peritoneal neutrophil influx (Fig. 8, B–D). In contrast, mice that were primed with LPS followed by an injection of C-16 lysoPAF displayed increased serum IL-1 $\beta$ , IL-18, and peritoneal neutrophil influx (Fig. 8, B–D). Administration of MCC950 blocked the elevation of serum IL-1 $\beta$ , IL-18, and peritoneal neutrophil influx (Fig. 8, B–D), suggesting that this activation was dependent on NLRP3. Using a genetic approach, we tested several gene deletion strains lacking components of the inflammasome. Deficiencies in *Nlrp3*, *Asc*, and *Casp1*, but not *Casp11*, caused reduced serum IL-1 $\beta$  and IL-18 in a similar manner as treatment with MCC950 (Fig. 8, F–H; and Fig. S5, A and B). As a control, serum TNF elevation was dependent on LPS priming alone, but not on lysoPAF, nor was it affected by the NLRP3 inflammasome (Fig. 8, E and I). Furthermore, *Il1r1*<sup>-/-</sup> mice, in which IL1 signaling is abolished, displayed reduced neutrophil flux (Fig. 8 J) in response to stimulation. Thus, lysoPAF, which does not activate PAFR, induces an NLRP3 inflammasome-dependent inflammatory response in vivo.

To further address the role of PAFR, we tested *Paf1r*<sup>-/-</sup> mice. LPS followed by PAF injection induced increased serum IL-1 $\beta$ , IL-18, and peritoneal neutrophil influx in *Paf1r*<sup>-/-</sup> mice (Fig. 8, K–M). This effect was dependent on NLRP3, since MCC950 blocked both of these events (Fig. 8, K–M). As a control, serum TNF elevation was dependent on LPS priming alone, but not on the NLRP3 inflammasome (Fig. 8 N). Consistently, LPS followed by PAF treatment induced comparable IL-1 $\beta$  and IL-18 detected in peritoneal lavage in WT and *Paf1r*<sup>-/-</sup> mice (Fig. 8, O and P).

Collectively, these data indicate that PAF and lysoPAF induce NLRP3 inflammasome activation in vivo in a PAFR-independent fashion.

## Discussion

In this study, a combination of genetic, pharmacologic, biochemical, and imaging approaches was used to reveal a novel biological function of PAF in NLRP3 inflammasome activation. In addition to NLRP3, the common inflammasome adaptor molecule, ASC, and the NLRP3-specific associated protein, NEK7, are both required for PAF-induced inflammasome activation. In addition to PAF, lysoPAF also activates NLRP3 inflammasome both in vitro and in vivo. PAF is a lipid mediator that elicits responses in a wide variety of cell types (Prescott et al., 2000). Since PAFR is the only known receptor for PAF, most PAF biofunction is thought to be attributable to PAFR. This report used multiple approaches including the use of PAFR nonbinding lysoPAF isoforms, PAFR gene deletion mice, and PAFR inhibitors to show that PAF-induced inflammasome activation is unexpectedly independent from PAFR. Although PAFR is important for most PAF functions, the role of PAFR was questioned in a previous study that showed eosinophil degranulation and cytokine release in response to PAF and lysoPAF occurring independently of PAFR, as revealed using PAFR antagonists or PAFR gene deletion (Dyer et al., 2010). While PAF binds PAFR but lysoPAF does not, both can activate the inflammasome; this fact may partially explain the ineffectiveness of PAFR antagonists or PAF-acetylhydrolase in several clinical trials (Spence et al., 1994; Dhainaut et al., 1998; Henig et al., 2000; Vincent et al., 2000; Johnson et al., 2001).

Despite extensive study, the precise mechanism of NLRP3 inflammasome activation remains elusive. Our work shows that PAF-activated NLRP3 inflammasome is dependent on potassium and calcium flux and is subjected to cAMP-PKA suppression, as increasing cAMP synthesis or inhibiting cAMP degradation suppressed NLRP3 inflammasome activation by PAF. Activation of cAMP-PKA has been shown to suppress only NLRP3 activity, but not NLR4, AIM2, or NLRP1 inflammasomes (Yan et al., 2015; Guo et al., 2016). This further corroborates the genetic data as well as the results from the use of the NLRP3 inhibitor MCC950 to support the conclusion that PAF specifically activates NLRP3 inflammasome.

PAFR belongs to a GPCR subtype that induces downstream calcium flux and PKC activation and also inhibits the synthesis of cAMP by ADCY. PKC inhibitors also potently suppressed NLRP3 activation by PAF, but we were not able to detect the PKC phosphorylation motif on NLRP3 upon inflammasome activation (unpublished data). In addition, lipid raft inhibitors can suppress NLRP3 inflammasome activation by PAF, suggesting that other GPCRs that use PKC and calcium signaling might account for this effect of PAF, although further studies are required to identify the specific pathway involved.

In summary, our study uncovered a phospholipid, PAF, serving as a damage-associated molecular pattern to activate the NLRP3 inflammasome. We showed that this biological activity contributes to the inflammatory pathways activated by PAF.

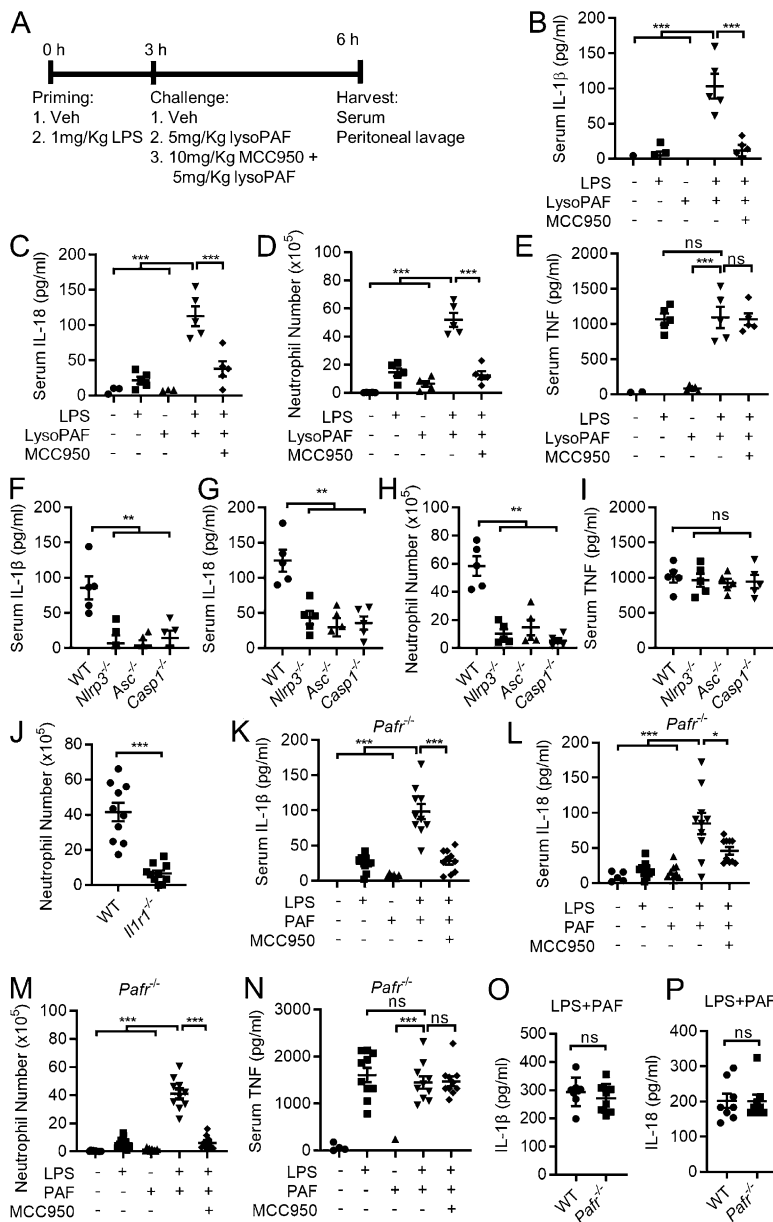


**Figure 8. PAF induces NLRP3 inflammasome activation in vivo independently of PAFR.** (A) Schematic representation of the in vivo experimental design. (B–E) Serum IL-1 $\beta$  by ELISA (B), serum IL-18 (C), peritoneal neutrophil influx (D), and serum TNF (E) from WT mice treated as depicted in A. (F–I) Serum IL-1 $\beta$  (F), IL-18 (G), peritoneal neutrophil influx (H), and serum TNF (I) from mice of indicated genotype challenged as depicted in A, but only with LPS followed by lysoPAF. (J–N) Serum IL-1 $\beta$  (J), IL-18 (K), peritoneal neutrophil influx (L), and serum TNF (M) from *Paf1r*<sup>-/-</sup> mice treated as in A, but with lysoPAF replaced with PAF. (O and P) IL-1 $\beta$  (O) and IL-18 ELISA (P) of peritoneal lavage in WT and *Paf1r*<sup>-/-</sup> mice after 3-h LPS treatment followed by 30-min PAF treatment. Veh, vehicle control. Data are presented as mean  $\pm$  SEM. Data in B–I are one representative experiment of three independent experiments. Data in J–N are pooled from three independent experiments. Data in O and P are pooled from two independent experiments. \*\*, P < 0.01; \*\*\*, P < 0.001. ns, not significant. One-way ANOVA (B–I and K–N); unpaired Student's t test (J, O, and P).

This represents a novel sequela of PAF and lysoPAF sensing and provides new insights regarding PAF-driven inflammation as distinct from PAFR stimulation.

## Materials and methods

### Mice

All animal protocols were approved by the Institutional Animal Care and Use Committee of the University of North Carolina at Chapel Hill in accordance with the National Institutes of Health Guide for the Care and Use of Laboratory Animals. All animal experiments were performed under specific pathogen-free conditions in sterile isolated caging using 6–8-wk-old mice. WT C57BL/6 mice were initially from the Jackson Laboratory. The *Nlrp1*<sup>-/-</sup>, *Nlrp3*<sup>-/-</sup>, *Nlrp6*<sup>-/-</sup>, *Nlr4*<sup>-/-</sup>, *Aim2*<sup>-/-</sup>, *Asc*<sup>-/-</sup>, *Casp1*<sup>-/-</sup> (*Ice*<sup>-/-</sup>-*Casp1*<sup>fl/fl</sup>), *Casp11*<sup>-/-</sup>, *Il1b*<sup>-/-</sup>, *Il18*<sup>-/-</sup>, *Nek7*<sup>-/-</sup>, *Gsdmd*<sup>-/-</sup>, *Paf1r*<sup>-/-</sup>, and ASC-citrine mice were all described previously

(Shornick et al., 1996; Ishii et al., 1998; Takeda et al., 1998; Mariathasan et al., 2004; Sutterwala et al., 2006; Kayagaki et al., 2011; Kovarova et al., 2012; Wilson et al., 2015; Shi et al., 2016; Tzeng et al., 2016; Patel and Kearney, 2017; Rauch et al., 2017). The mice were received backcrossed onto C57BL/6 background, or additional backcrossing schemes to C57BL/6 were performed as follows: *Nlrp1*<sup>-/-</sup> for three generations, *Nlrp3*<sup>-/-</sup> for at least six generations, *Aim2*<sup>-/-</sup> for nine generations, *Nlrp6*<sup>-/-</sup> for two generations, *Nlr4*<sup>-/-</sup> for at least three generations, *Asc*<sup>-/-</sup> for at least four generations, *Casp11*<sup>-/-</sup> for three generations, *Il1b*<sup>-/-</sup> for at least six generations, and *Il18*<sup>-/-</sup> for three generations. *P2x7*<sup>-/-</sup> and *Il1r1*<sup>-/-</sup> (#003245; Jackson Laboratory) mice were maintained on a B6.129 background. *Paf1r*<sup>-/-</sup> mice were housed at the University of Alabama at Birmingham. Institutionally housed age- and sex-matched C57BL/6J mice or B6.129 mice from the same facility were used as controls. No randomization of the allocation of animals to experimental groups was performed.

## Cell culture

BMDMs and BMDCs were generated by flushing murine femurs, and red blood cells were removed by ammonium-chloride-potassium lysis. BMDMs were differentiated in the presence of L-929 conditioned medium (50% DMEM, 20% FBS, 30% L-929 medium, and 1% penicillin/streptomycin) for 5 d. BMDCs were differentiated in RPMI-1640 culture medium containing 10% FBS, 50  $\mu$ M  $\beta$ -mercaptoethanol, 40 ng/ml GM-CSF, and 1% penicillin/streptomycin for 7 d. DMEM (#11995065) and RPMI-1640 (#11875-093) were purchased from Gibco (Thermo Fisher Scientific). FBS (#F2442) was purchased from Sigma-Aldrich. Murine GM-CSF (#315-03) was purchased from Peprotech. All cells were grown in a 37°C incubator supplied with 5% CO<sub>2</sub>.

Human dendritic cells were generated from patients enrolled in a clinical trial approved by the University of North Carolina Office of Human Research Ethics (Institutional Review Board Study #05-2860) after informed consent was provided. The cells were provided as deidentified samples for this study. Primary human dendritic cells were generated by culturing CD34<sup>+</sup>-selected cells from peripheral blood in the presence of stem cell factor (50 ng/ml), Flt3L (100 ng/ml), and GM-CSF (800 U/ml) for 72 h. The pre-dendritic cells (preDCs) were expanded in GM-CSF (800 U/ml; Leukine Sanofi-Genzyme) and IL-4 (500 U/ml) in AIM V medium (#0870112BK; Thermo Fisher Scientific) with 10% human AB serum (GemCell #100-512; Gemini Bio-Products) for 9 d in 6-well cluster plates (Corning Costar, #3471; Thermo Fisher Scientific). Stem cell factor (#300-07), Flt3L (#300-19), and IL-4 (#200-04) were obtained from Peprotech. Human macrophages were generated from human peripheral blood monocytes isolated from leukapheresis buffy coats (Gulf Coast Regional Blood Center). Peripheral blood monocytes were suspended in AIM V medium with 10% human serum and allowed to attach to T75 flasks for 2 h. The adherent cells were washed with warm AIM V medium and cultured in AIM V medium with 10% human serum plus 100 ng/ml GM-CSF for 6 d.

## Reagents and antibodies

Human IL-1 $\beta$  (#557953), mouse IL-1 $\beta$  (#559603), and mouse TNF (#555268) ELISA kits were obtained from BD Biosciences. Mouse IL-18 (#7625) ELISA kit was from R&D Systems. LPS-EB Ultra-pure (#tlrl-3pelps), nigericin (#tlrl-nig), poly(dA:dT) (#tlrl-patn), flagellin from *Salmonella typhimurium* (#tlrl-epstfla), MSU crystals (#tlrl-msu), nano-SiO<sub>2</sub> (#tlrl-sio), and mouse TLR1-9 agonist kit (#tlrl-kitlmw) were purchased from InvivoGen. Alum (#77161) was obtained from Thermo Fisher Scientific; PAF (C16; #2940) and butenoyl PAF (#60929) from Tocris (Bio-Techne); and PAF C-18 (#sc-205421, #sc-201017), PAF C-18:1 (#sc-201019), butanoyl PAF (#sc-221386), Ginkgolide B (#sc-201037), WEB-2086 (#sc-201007), (2R,4R)-APDC (#sc-202408), and Zardaverine (#sc-201208) from Santa Cruz Biotechnology. C18:1 LysoPAF (#878126P) was from Avanti Polar Lipids; LysoPAF C-16 (#60906), LysoPAF C18 (#60916), NAC (#20261), m-3M3FBS (#16867), U73122 (#70740), A-804598 (#21256), A-740003 (#21256), VAS2870 (#19205), Ro 20-1724 (#18272), and forskolin (#11018) from Cayman Chemical; and zYVAD-fmk (#ALX-260-154-R100), zVAD-FMK (#ALX-260-138-R100), Mitotempo (#ALX-430-150-M005), DPI (#ALX-270-003), Ca-

074-Me (#BML-PI126-0001), BAPTA-AM (#BML-CA411-0025), and 2-APB (#ALX-400-045-M100) from Enzo Life Sciences. Apyrase (#M0398S) was from New England Biolabs; uricase (#ENZ-312) from ProSpec; MCC950 (#AG-CR1-3615-M001) from Adipogen; and methyl- $\beta$ -cyclodextrin (#332615-5G) and Filipin III (#F4767-1MG) from Sigma-Aldrich.

## Cell stimulation

After differentiation, macrophages were reseeded overnight in DMEM with 10% FBS, and DCs were seeded in RPMI-1640 supplemented with 10% FBS. 250,000 cells per well in a 96-well plate or 500,000 cells per well in a 24-well plate were seeded. The cells were primed with 300 ng/ml LPS for 3–4 h, washed with PBS, and then stimulated in serum-free DMEM or RPMI-1640 using inflammasome agonists or inhibitors.

For priming with TLR ligands, BMDMs were treated with 1  $\mu$ g/ml Pam3CSK4 (TLR1/2), 10<sup>7</sup>/ml HKLM (TLR2), 1  $\mu$ g/ml poly(I:C) (HMW; TLR3), 1  $\mu$ g/ml LPS-EK (TLR4), 1  $\mu$ g/ml FLA-ST (TLR5), 1  $\mu$ g/ml FSL-1 (TLR2/6), 1  $\mu$ g/ml ssRNA40 (TLR7), or 200 ng/ml ODN1826 (TLR9) for 3 h. All agonists (#tlrl-kitlmw kit) used here were from InvivoGen.

For inflammasome activation, cells were treated with 25, 50, or 100  $\mu$ M PAF, lysoPAF, or PAF-like lipid; 5, 10, or 40  $\mu$ M nigericin; 5 or 10 mM ATP; 300  $\mu$ g/ml silica; 300  $\mu$ g/ml alum; or 300  $\mu$ g/ml MSU for 0.5–6 h. For each well of a 96-well plate, 0.2  $\mu$ g poly(dA:dT) (final concentration at 2 ng/ $\mu$ l) was transfected with 0.5  $\mu$ l lipofectamine 2000 (#11668027; Thermo Fisher Scientific); 100 ng flagellin (final concentration at 1 ng/ $\mu$ l) was transfected with 1  $\mu$ l DOTAP (1,2-dioleoyl-3-trimethylammonium propane; #11202375001; Roche); and 100 ng LPS (final concentration at 1 ng/ $\mu$ l) was transfected with 0.5  $\mu$ l FuGENE HD (E2311; Promega). For each well of a 96-well plate, 1.3092  $\mu$ g PAF was transfected with 0.5  $\mu$ l lipofectamine 2000 or 1  $\mu$ l DOTAP. The final culture media volume was 100  $\mu$ l per well, so the PAF concentration was 25  $\mu$ M. PAF alone at 25  $\mu$ M or transfection reagent alone was used as a control. Additionally, m-3M3FBS (50 or 200  $\mu$ M) was used to activate inflammasome.

For inflammasome inhibition, MCC950 (50, 500, or 5,000 nM), zVAD (10 or 50  $\mu$ M), zYVAD (10 or 50  $\mu$ M), Ginkgolide B (10, 50, or 100  $\mu$ M), WEB-2086 (10, 50, or 100  $\mu$ M), (2R,4R)-APDC (10 or 50  $\mu$ M), Mitotempo (100 or 500  $\mu$ M), DPI (5 or 25  $\mu$ M), NAC (5 or 25 mM), BAPTA-AM (10 or 20  $\mu$ M), 2-APB (20 or 100  $\mu$ M), U73122 (2 or 10  $\mu$ M), aKCl (25 or 50 mM), M $\beta$ CD (5 or 15 mM), and Filipin III (2.5 or 12.5  $\mu$ g/ml), CA-074-ME (10 and 20  $\mu$ M), zardaverine (100 or 250  $\mu$ M), ro-20-1724 (100 or 250  $\mu$ M), forskolin (25 or 100  $\mu$ M), A-804598 (100  $\mu$ M), A-740003 (100  $\mu$ M), apyrase (1 U/ml), uricase (1 U/ml), and VAS2870 (1 or 5  $\mu$ M) were used. The inhibitors were individually added with agonists to avoid the potential impact of inhibitor on priming. DMEM (high glucose, no glutamine; #11960044; Gibco) or DMEM (high glucose, no glutamine, and no calcium; #21068028; Gibco) was used for calcium depletion experiments. Primary human cells were primed with 20 ng/ml LPS in AIM V medium with 10% human AB serum for 3 h, then washed with PBS and stimulated with 25 or 50  $\mu$ M PAF in serum-free AIM V medium.

### ASC oligomerization assay

ASC oligomerization assays were performed as previously described (Zhao et al., 2014). Disuccinimidyl suberate (#PI21658) was from Thermo Fisher Scientific.

### LDH assay

LDH release was measured using a cytotoxicity detection kit (#11644793001; Sigma-Aldrich) according to the manufacturer's instructions.

### Western blotting

The cells were lysed with radioimmunoprecipitation assay buffer (BP-116TX; Boston Bio Products) plus protease inhibitor (cOmplete, #11697498001; Sigma-Aldrich) and phosphatase inhibitor (PhosSTOP, #4906845001; Sigma-Aldrich) for 30 min on ice. Cell lysates or supernatants were mixed with SDS loading buffer and denatured at 95°C for 15 min. Then the samples were subjected to 4–12% NuPAGE (Invitrogen) electrophoresis and transferred to nitrocellulose membrane (#1620112; Bio-Rad). The membranes were blocked with 5% milk in Tris-buffered saline/Tween buffer for 1 h. The following antibodies were used at 1:2,000 dilution: anti-IL-1 $\beta$  (AF401-NA; R&D Systems), anti-NLRP3 (AG-20B-0014-C100; Adipogen), anti-caspase-1 p10 (AG-20B-0044-C100; Adipogen), anti-caspase-1 p20 (AG-20B-0042-C100; Adipogen), anti-ASC (AG-25B-0006-C100; Adipogen), and anti-GSDMD (ab209845; Abcam). The following secondary antibodies were used at 1:5,000 dilution: anti- $\beta$ -actin (sc-1615; HRP conjugate; Santa Cruz Biotechnology), goat anti-rabbit HRP (111-035-144; Jackson ImmunoResearch Laboratories), and goat anti-mouse HRP (115-035-146; Jackson ImmunoResearch Laboratories). Proteins were detected using Pico or Femto Chemiluminescent reagents (#34577 or #34095; Thermo Fisher Scientific).

### Confocal microscopy imaging

BMDMs from ASC-citrine mice were seeded on glass coverslips in a 24-well plate. Cells were treated with 300 ng/ml LPS for 3 h followed by vehicle control, C16 PAF (25  $\mu$ M), or nigericin (10  $\mu$ M) for 3 h. Cells were fixed with 4% paraformaldehyde and stained with DAPI (#D1306; Thermo Fisher Scientific), followed by imaging on a Zeiss LSM 710 laser-scanning confocal microscope. Images were acquired by Zen software at 40 $\times$ .

### In vivo mouse model

Mice were primed via i.p. injection with 1 mg/kg LPS or vehicle control (PBS) for 3 h. Mice were then challenged (i.p.) with 5 mg/kg C16 lysoPAF, 5 mg/kg C16 PAF, or vehicle control (PBS) as indicated. MCC950 (10 mg/kg) was injected i.p. together with C16 lysoPAF or C16 PAF. The serum was collected 6 h after challenge for cytokine ELISA. For measuring peritoneal neutrophil influx, mice were sacrificed at 6 h after challenge, and the peritoneal cavity was rinsed with 2 ml cold PBS to collect infiltrate. Total cells were counted, blocked by anti-mouse CD16/32 antibody (101302; BioLegend), and then stained with Ly-6G antibody (127601; BioLegend) and CD11b antibody (101205; BioLegend) in FACS buffer (PBS with 2% FBS). All data were collected using a Cyan ADP (Beckman Coulter) or Becton

Dickinson LSRII (BD Biosciences) flow cytometer and analyzed using FlowJo software (TreeStar). Ly-6G and CD11b double-positive cells were gated as neutrophils. For comparing WT and *Pafr*<sup>-/-</sup> mice, mice were primed via i.p. injection with 1 mg/kg LPS for 3 h, followed by i.p. injection of 5 mg/kg C16 PAF for 0.5 h. Peritoneal lavage was collected and analyzed.

### Statistical analysis

Statistical analyses were performed using Prism 7.0 (GraphPad). Data are presented as mean  $\pm$  SD or mean  $\pm$  SEM as denoted in figure legends. Unpaired Student's *t* tests were used for two-group analysis. If multiple subgroups were compared between two groups, the Holm–Sidak method was used for correcting the *P* value. One-way ANOVA followed by Dunnett's post hoc analysis was used for multigroup comparisons. In all tests, *P* values or adjusted *P* values <0.05 were considered statistically significant.

### Online supplemental material

Fig. S1 shows that transfected PAF does not induce IL-1 $\beta$  secretion. Fig. S2 shows that PAF-induced cytotoxicity in BMDMs is independent of the NLRP3 inflammasome in most assay conditions. Fig. S3 shows that PAF-induced NLRP3 inflammasome activation requires calcium and potassium flux, but not ROS and lysosomal cathepsin. Fig. S4 shows that PAF-induced NLRP3 inflammasome activation is independent of ATP and uric acid release, inhibited by increasing cAMP, and reduced by lipid raft inhibitors. Fig. S5 shows that PAF-induced NLRP3 inflammasome activation in vivo is independent of caspase-11.

### Acknowledgments

We sincerely thank Dr. Takao Shimizu (University of Tokyo, Tokyo, Japan) for approval to use the *Pafr*<sup>-/-</sup> mice, Dr. John F. Kearney (University of Alabama at Birmingham, Birmingham, AL) for providing *Pafr*<sup>-/-</sup> mice, and Dr. Russell Vance (University of California, Berkeley, Berkeley, CA) for approval and Dr. Edward Miao (University of North Carolina Chapel Hill, Chapel Hill, NC) for sharing *Gsdmd*<sup>-/-</sup> mice.

This work was supported by National Institutes of Health grants R01 AI029564, R01 CA156330, R35 CA232109, and P01 DK094779 to J.P.-Y. Ting; AI14782 and U01 AI100005 to Dr. John F. Kearney (University of Alabama at Birmingham); and AI1007051 to J.S. New. The University of North Carolina Flow Cytometry Core Facility and Microscopy Services Laboratory is supported by the National Institutes of Health P30 CA016086 Cancer Center Core Support Grant to the University of North Carolina Lineberger Comprehensive Cancer Center.

The authors declare no competing financial interests.

Author contributions: M. Deng and J.P.-Y. Ting designed the study. J.P.-Y. Ting supervised the project. M. Deng and J.P.-Y. Ting wrote the manuscript with input from J.W. Tam, B.M. Johnson, and W.J. Brickey. M. Deng, H. Guo, J.W. Tam, and B.M. Johnson performed the experiments and analyzed the data. D. Golenbock generated and provided bone marrow from ASC-citrine mice. B.H. Koller generated, bred, and provided the *P2x7*<sup>-/-</sup> mice. H. Shi and B. Beutler generated bone marrow

from *Nek7*<sup>-/-</sup> mice. J.S. New and A. Lenox from Dr. John Kearney's laboratory, University of Alabama at Birmingham, bred and provided the *Pafr*<sup>-/-</sup> mice. Other mice were bred and provided by W.J. Brickley. K. McKinnon generated and provided human cells.

Submitted: 16 January 2019

Revised: 9 July 2019

Accepted: 4 September 2019

## References

- Agostini, L., F. Martinon, K. Burns, M.F. McDermott, P.N. Hawkins, and J. Tschopp. 2004. NALP3 forms an IL-1 $\beta$ -processing inflammasome with increased activity in Muckle-Wells autoinflammatory disorder. *Immunity*. 20:319–325. [https://doi.org/10.1016/S1074-7613\(04\)00046-9](https://doi.org/10.1016/S1074-7613(04)00046-9)
- Bazan, N.G. 2003. Synaptic lipid signaling: significance of polyunsaturated fatty acids and platelet-activating factor. *J. Lipid Res.* 44:2221–2233. <https://doi.org/10.1194/jlr.R300013-JLR200>
- Benveniste, J., P.M. Henson, and C.G. Cochrane. 1972. Leukocyte-dependent histamine release from rabbit platelets. The role of IgE, basophils, and a platelet-activating factor. *J. Exp. Med.* 136:1356–1377. <https://doi.org/10.1084/jem.136.6.1356>
- Bürckstümmer, T., C. Baumann, S. Blüml, E. Dixit, G. Dürnberger, H. Jahn, M. Planyavsky, M. Bilban, J. Colinge, K.L. Bennett, and G. Superti-Furga. 2009. An orthogonal proteomic-genomic screen identifies AIM2 as a cytoplasmic DNA sensor for the inflammasome. *Nat. Immunol.* 10:266–272. <https://doi.org/10.1038/ni.1702>
- Callea, L., M. Arese, A. Orlandini, C. Bargnani, A. Priori, and F. Bussolino. 1999. Platelet activating factor is elevated in cerebral spinal fluid and plasma of patients with relapsing-remitting multiple sclerosis. *J. Neuroimmunol.* 94:212–221. [https://doi.org/10.1016/S0165-5728\(98\)00246-X](https://doi.org/10.1016/S0165-5728(98)00246-X)
- Coll, R.C., A.A.B. Robertson, J.J. Chae, S.C. Higgins, R. Muñoz-Planillo, M.C. Inerra, I. Vetter, L.S. Dungan, B.G. Monks, A. Stutz, et al. 2015. A small-molecule inhibitor of the NLRP3 inflammasome for the treatment of inflammatory diseases. *Nat. Med.* 21:248–255. <https://doi.org/10.1038/nm.3806>
- Coll, R.C., J.R. Hill, C.J. Day, A. Zamoshnikova, D. Boucher, N.L. Massey, J.L. Chitty, J.A. Fraser, M.P. Jennings, A.A.B. Robertson, and K. Schroder. 2019. MCC950 directly targets the NLRP3 ATP-hydrolysis motif for inflammasome inhibition. *Nat. Chem. Biol.* 15:556–559. <https://doi.org/10.1038/s41589-019-0277-7>
- Davis, B.K., H. Wen, and J.P. Ting. 2011. The inflammasome NLRs in immunity, inflammation, and associated diseases. *Annu. Rev. Immunol.* 29:707–735. <https://doi.org/10.1146/annurev-immunol-031210-101405>
- Deng, M., Y. Tang, W. Li, X. Wang, R. Zhang, X. Zhang, X. Zhao, J. Liu, C. Tang, Z. Liu, et al. 2018. The Endotoxin Delivery Protein HMGB1 Mediates Caspase-11-Dependent Lethality in Sepsis. *Immunity*. 49:740–753.e747.
- Dhainaut, J.F., A. Tenaillon, M. Hemmer, P. Damas, Y. Le Tulzo, P. Radermacher, M.D. Schaller, J.P. Sollet, M. Wolff, L. Holzappel, et al. 1998. Confirmatory platelet-activating factor receptor antagonist trial in patients with severe gram-negative bacterial sepsis: a phase III, randomized, double-blind, placebo-controlled, multicenter trial. BN 52021 Sepsis Investigator Group. *Crit. Care Med.* 26:1963–1971. <https://doi.org/10.1097/00003246-199812000-00021>
- Dyer, K.D., C.M. Percopo, Z. Xie, Z. Yang, J.D. Kim, F. Davoine, P. Lacy, K.M. Druey, R. Moqbel, and H.F. Rosenberg. 2010. Mouse and human eosinophils degranulate in response to platelet-activating factor (PAF) and lysoPAF via a PAF-receptor-independent mechanism: evidence for a novel receptor. *J. Immunol.* 184:6327–6334. <https://doi.org/10.4049/jimmunol.0904043>
- Elinav, E., T. Strowig, A.L. Kau, J. Henao-Mejia, C.A. Thaiss, C.J. Booth, D.R. Peaper, J. Bertin, S.C. Eisenbarth, J.I. Gordon, and R.A. Flavell. 2011. NLRP6 inflammasome regulates colonic microbial ecology and risk for colitis. *Cell*. 145:745–757. <https://doi.org/10.1016/j.cell.2011.04.022>
- Evavold, C.L., J. Ruan, Y. Tan, S. Xia, H. Wu, and J.C. Kagan. 2018. The pore-forming protein gasdermin D regulates interleukin-1 secretion from living macrophages. *Immunity*. 48:35–44.e6. <https://doi.org/10.1016/j.immuni.2017.11.013>
- Fernandes-Alnemri, T., J.W. Yu, P. Datta, J. Wu, and E.S. Alnemri. 2009. AIM2 activates the inflammasome and cell death in response to cytoplasmic DNA. *Nature*. 458:509–513. <https://doi.org/10.1038/nature07710>
- Franchi, L., A. Amer, M. Body-Malapel, T.-D. Kanneganti, N. Ozören, R. Jagirdar, N. Inohara, P. Vandenabeele, J. Bertin, A. Coyle, et al. 2006. Cytosolic flagellin requires Ipaf for activation of caspase-1 and interleukin 1 $\beta$  in salmonella-infected macrophages. *Nat. Immunol.* 7:576–582. <https://doi.org/10.1038/ni1346>
- Groß, C.J., R. Mishra, K.S. Schneider, G. Médard, J. Wettmarshausen, D.C. Dittlein, H. Shi, O. Gorka, P.-A. Koenig, S. Fromm, et al. 2016. K+ efflux-independent NLRP3 inflammasome activation by small molecules targeting mitochondria. *Immunity*. 45:761–773. <https://doi.org/10.1016/j.immuni.2016.08.010>
- Guo, C., S. Xie, Z. Chi, J. Zhang, Y. Liu, L. Zhang, M. Zheng, X. Zhang, D. Xia, Y. Ke, et al. 2016. Bile acids control inflammation and metabolic disorder through inhibition of NLRP3 inflammasome. *Immunity*. 45:802–816. <https://doi.org/10.1016/j.immuni.2016.09.008>
- Guo, H., J.B. Callaway, and J.P. Ting. 2015. Inflammasomes: mechanism of action, role in disease, and therapeutics. *Nat. Med.* 21:677–687. <https://doi.org/10.1038/nm.3893>
- Hagar, J.A., D.A. Powell, Y. Achoui, R.K. Ernst, and E.A. Miao. 2013. Cytoplasmic LPS activates caspase-11: implications in TLR4-independent endotoxic shock. *Science*. 341:1250–1253. <https://doi.org/10.1126/science.1240988>
- Hara, H., S.S. Seregin, D. Yang, K. Fukase, M. Chamailard, E.S. Alnemri, N. Inohara, G.Y. Chen, and G. Núñez. 2018. The NLRP6 inflammasome recognizes lipoteichoic acid and regulates gram-positive pathogen infection. *Cell*. 175:1651–1664.e14. <https://doi.org/10.1016/j.cell.2018.09.047>
- He, W.-T., H. Wan, L. Hu, P. Chen, X. Wang, Z. Huang, Z.-H. Yang, C.-Q. Zhong, and J. Han. 2015. Gasdermin D is an executor of pyroptosis and required for interleukin-1 $\beta$  secretion. *Cell Res*. 25:1285–1298. <https://doi.org/10.1038/cr.2015.139>
- He, Y., M.Y. Zeng, D. Yang, B. Motro, and G. Núñez. 2016. NEK7 is an essential mediator of NLRP3 activation downstream of potassium efflux. *Nature*. 530:354–357. <https://doi.org/10.1038/nature16959>
- Henig, N.R., M.L. Aitken, M.C. Liu, A.S. Yu, and W.R. Henderson Jr. 2000. Effect of recombinant human platelet-activating factor-acetylhydrolase on allergen-induced asthmatic responses. *Am. J. Respir. Crit. Care Med.* 162:523–527. <https://doi.org/10.1164/ajrccm.162.2.9911084>
- Hoffman, H.M., J.L. Mueller, D.H. Broide, A.A. Wanderer, and R.D. Kolodner. 2001. Mutation of a new gene encoding a putative pyrin-like protein causes familial cold autoinflammatory syndrome and Muckle-Wells syndrome. *Nat. Genet.* 29:301–305. <https://doi.org/10.1038/ng756>
- Hornung, V., A. Ablasser, M. Charrel-Dennis, F. Bauernfeind, G. Horvath, D.R. Caffrey, E. Latz, and K.A. Fitzgerald. 2009. AIM2 recognizes cytosolic dsDNA and forms a caspase-1-activating inflammasome with ASC. *Nature*. 458:514–518. <https://doi.org/10.1038/nature07725>
- Ishii, S., and T. Shimizu. 2000. Platelet-activating factor (PAF) receptor and genetically engineered PAF receptor mutant mice. *Prog. Lipid Res.* 39:41–82. [https://doi.org/10.1016/S0163-7827\(99\)00016-8](https://doi.org/10.1016/S0163-7827(99)00016-8)
- Ishii, S., T. Kuwaki, T. Nagase, K. Maki, F. Tashiro, S. Sunaga, W.-H. Cao, K. Kume, Y. Fukuchi, K. Ikuta, et al. 1998. Impaired anaphylactic responses with intact sensitivity to endotoxin in mice lacking a platelet-activating factor receptor. *J. Exp. Med.* 187:1779–1788. <https://doi.org/10.1084/jem.187.11.1779>
- Johnson, C.D., A.N. Kingsnorth, C.W. Imrie, M.J. McMahon, J.P. Neoptolemos, C. McKay, S.K. Toh, P. Skaife, P.C. Leeder, P. Wilson, et al. 2001. Double blind, randomised, placebo controlled study of a platelet activating factor antagonist, lexipafant, in the treatment and prevention of organ failure in predicted severe acute pancreatitis. *Gut*. 48:62–69. <https://doi.org/10.1136/gut.48.1.62>
- Kayagaki, N., S. Warming, M. Lamkanfi, L. Vande Walle, S. Louie, J. Dong, K. Newton, Y. Qu, J. Liu, S. Heldens, et al. 2011. Non-canonical inflammasome activation targets caspase-11. *Nature*. 479:117–121. <https://doi.org/10.1038/nature10558>
- Kayagaki, N., M.T. Wong, I.B. Stowe, S.R. Ramani, L.C. Gonzalez, S. Akashi-Takamura, K. Miyake, J. Zhang, W.P. Lee, A. Muszynski, et al. 2013. Noncanonical inflammasome activation by intracellular LPS independent of TLR4. *Science*. 341:1246–1249. <https://doi.org/10.1126/science.1240248>
- Kayagaki, N., I.B. Stowe, B.L. Lee, K. O'Rourke, K. Anderson, S. Warming, T. Cuellar, B. Haley, M. Roose-Girma, Q.T. Phung, et al. 2015. Caspase-11 cleaves gasdermin D for non-canonical inflammasome signalling. *Nature*. 526:666–671. <https://doi.org/10.1038/nature15541>

- Kerur, N., M.V. Veettil, N. Sharma-Walia, V. Bottero, S. Sadagopan, P. Otageri, and B. Chandran. 2011. IFI16 acts as a nuclear pathogen sensor to induce the inflammasome in response to Kaposi Sarcoma-associated herpesvirus infection. *Cell Host Microbe*. 9:363–375. <https://doi.org/10.1016/j.chom.2011.04.008>
- Khare, S., A. Dorfleutner, N.B. Bryan, C. Yun, A.D. Radian, L. de Almeida, Y. Rojanasakul, and C. Stehlik. 2012. An NLRP7-containing inflammasome mediates recognition of microbial lipopeptides in human macrophages. *Immunity*. 36:464–476. <https://doi.org/10.1016/j.immuni.2012.02.001>
- Kovarova, M., P.R. Hesker, L. Jania, M. Nguyen, J.N. Snouwaert, Z. Xiang, S.E. Lommatzsch, M.T. Huang, J.P. Ting, and B.H. Koller. 2012. NLRP1-dependent pyroptosis leads to acute lung injury and morbidity in mice. *J. Immunol.* 189:2006–2016. <https://doi.org/10.4049/jimmunol.1201065>
- Lee, G.-S., N. Subramanian, A.I. Kim, I. Aksentijevich, R. Goldbach-Mansky, D.B. Sacks, R.N. Germain, D.L. Kastner, and J.J. Chae. 2012. The calcium-sensing receptor regulates the NLRP3 inflammasome through Ca<sup>2+</sup> and cAMP. *Nature*. 492:123–127. <https://doi.org/10.1038/nature11588>
- Mangan, M.S.J., E.J. Olhava, W.R. Roush, H.M. Seidel, G.D. Glick, and E. Latz. 2018. Targeting the NLRP3 inflammasome in inflammatory diseases. *Nat. Rev. Drug Discov.* 17:588–606. <https://doi.org/10.1038/nrd.2018.97>
- Mariathasan, S., K. Newton, D.M. Monack, D. Vucic, D.M. French, W.P. Lee, M. Roose-Girma, S. Erickson, and V.M. Dixit. 2004. Differential activation of the inflammasome by caspase-1 adaptors ASC and Ipaf. *Nature*. 430:213–218. <https://doi.org/10.1038/nature02664>
- Mariathasan, S., D.S. Weiss, K. Newton, J. McBride, K. O'Rourke, M. Roose-Girma, W.P. Lee, Y. Weinrauch, D.M. Monack, and V.M. Dixit. 2006. Cryopyrin activates the inflammasome in response to toxins and ATP. *Nature*. 440:228–232. <https://doi.org/10.1038/nature04515>
- Martinon, F., K. Burns, and J. Tschopp. 2002. The inflammasome: a molecular platform triggering activation of inflammatory caspases and processing of proIL- $\beta$ . *Mol. Cell*. 10:417–426. [https://doi.org/10.1016/S1097-2765\(02\)00599-3](https://doi.org/10.1016/S1097-2765(02)00599-3)
- Martinon, F., V. Pétrilli, A. Mayor, A. Tardivel, and J. Tschopp. 2006. Gout-associated uric acid crystals activate the NALP3 inflammasome. *Nature*. 440:237–241. <https://doi.org/10.1038/nature04516>
- Miao, E.A., C.M. Alpuche-Aranda, M. Dors, A.E. Clark, M.W. Bader, S.I. Miller, and A. Aderem. 2006. Cytoplasmic flagellin activates caspase-1 and secretion of interleukin 1 $\beta$  via Ipaf. *Nat. Immunol.* 7:569–575. <https://doi.org/10.1038/ni1344>
- Montrucchio, G., F. Mariano, P.L. Cavalli, C. Tetta, G. Viglino, G. Emanuelli, and G. Camussi. 1989. Platelet activating factor is produced during infectious peritonitis in CAPD patients. *Kidney Int.* 36:1029–1036. <https://doi.org/10.1038/ki.1989.297>
- Moon, J.S., K. Nakahira, K.P. Chung, G.M. DeNicola, M.J. Koo, M.A. Pabón, K.T. Rooney, J.H. Yoon, S.W. Ryter, H. Stout-Delgado, and A.M. Choi. 2016. NOX4-dependent fatty acid oxidation promotes NLRP3 inflammasome activation in macrophages. *Nat. Med.* 22:1002–1012. <https://doi.org/10.1038/nm.4153>
- Mortimer, L., F. Moreau, J.A. MacDonal, and K. Chadee. 2016. NLRP3 inflammasome inhibition is disrupted in a group of auto-inflammatory disease CAPS mutations. *Nat. Immunol.* 17:1176–1186. <https://doi.org/10.1038/ni.3538>
- Muñoz-Planillo, R., P. Kuffa, G. Martínez-Colón, B.L. Smith, T.M. Rajendiran, and G. Núñez. 2013. K<sup>+</sup> efflux is the common trigger of NLRP3 inflammasome activation by bacterial toxins and particulate matter. *Immunity*. 38:1142–1153. <https://doi.org/10.1016/j.immuni.2013.05.016>
- Patel, P.S., and J.F. Kearney. 2017. CD36 and Platelet-Activating Factor Receptor Promote House Dust Mite Allergy Development. *J. Immunol.* 199:1184–1195. <https://doi.org/10.4049/jimmunol.1700034>
- Piccini, A., S. Carta, S. Tassi, D. Lasiglié, G. Fossati, and A. Rubartelli. 2008. ATP is released by monocytes stimulated with pathogen-sensing receptor ligands and induces IL-1 $\beta$  and IL-18 secretion in an autocrine way. *Proc. Natl. Acad. Sci. USA*. 105:8067–8072. <https://doi.org/10.1073/pnas.0709684105>
- Prescott, S.M., G.A. Zimmerman, D.M. Stafforini, and T.M. McIntyre. 2000. Platelet-activating factor and related lipid mediators. *Annu. Rev. Biochem.* 69:419–445. <https://doi.org/10.1146/annurev.biochem.69.1.419>
- Rauch, I., K.A. Deets, D.X. Ji, J. von Moltke, J.L. Tenthorey, A.Y. Lee, N.H. Philip, J.S. Ayres, I.E. Brodsky, K. Gronert, and R.E. Vance. 2017. NAIP-NLRC4 inflammasomes coordinate intestinal epithelial cell expulsion with eicosanoid and IL-18 release via activation of caspase-1 and-8. *Immunity*. 46:649–659. <https://doi.org/10.1016/j.immuni.2017.03.016>
- Rossol, M., M. Pierer, N. Raulien, D. Quandt, U. Meusch, K. Rothe, K. Schuberth, T. Schöneberg, M. Schaefer, U. Krügel, et al. 2012. Extracellular Ca<sup>2+</sup> is a danger signal activating the NLRP3 inflammasome through G protein-coupled calcium sensing receptors. *Nat. Commun.* 3:1329. <https://doi.org/10.1038/ncomms2339>
- Schmid-Burgk, J.L., D. Chauhan, T. Schmidt, T.S. Ebert, J. Reinhardt, E. Endl, and V. Hornung. 2016. A genome-wide CRISPR (clustered regularly interspaced short palindromic repeats) screen identifies NEK7 as an essential component of NLRP3 inflammasome activation. *J. Biol. Chem.* 291:103–109. <https://doi.org/10.1074/jbc.C115.700492>
- Schneider, K.S., C.J. Groß, R.F. Dreier, B.S. Saller, R. Mishra, O. Gorka, R. Heilig, E. Meunier, M.S. Dick, T. Čiković, et al. 2017. The inflammasome drives GSDMD-independent secondary pyroptosis and IL-1 release in the absence of caspase-1 protease activity. *Cell Reports*. 21:3846–3859. <https://doi.org/10.1016/j.celrep.2017.12.018>
- Shi, H., Y. Wang, X. Li, X. Zhan, M. Tang, M. Fina, L. Su, D. Pratt, C.H. Bu, S. Hildebrand, et al. 2016. NLRP3 activation and mitosis are mutually exclusive events coordinated by NEK7, a new inflammasome component. *Nat. Immunol.* 17:250–258. <https://doi.org/10.1038/ni.3333>
- Shi, J., Y. Zhao, Y. Wang, W. Gao, J. Ding, P. Li, L. Hu, and F. Shao. 2014. Inflammatory caspases are innate immune receptors for intracellular LPS. *Nature*. 514:187–192. <https://doi.org/10.1038/nature13683>
- Shi, J., Y. Zhao, K. Wang, X. Shi, Y. Wang, H. Huang, Y. Zhuang, T. Cai, F. Wang, and F. Shao. 2015. Cleavage of GSDMD by inflammatory caspases determines pyroptotic cell death. *Nature*. 526:660–665. <https://doi.org/10.1038/nature15514>
- Shi, Y., J.E. Evans, and K.L. Rock. 2003. Molecular identification of a danger signal that alerts the immune system to dying cells. *Nature*. 425:516–521. <https://doi.org/10.1038/nature01991>
- Shornick, L.P., P. De Togni, S. Mariathasan, J. Goellner, J. Strauss-Schoenberger, R.W. Karr, T.A. Ferguson, and D.D. Chaplin. 1996. Mice deficient in IL-1 $\beta$  manifest impaired contact hypersensitivity to trinitrochlorobenzene. *J. Exp. Med.* 183:1427–1436. <https://doi.org/10.1084/jem.183.4.1427>
- Spence, D.P., S.L. Johnston, P.M. Calverley, P. Dhillon, C. Higgins, E. Ramahadany, S. Turner, A. Winning, J. Winter, and S.T. Holgate. 1994. The effect of the orally active platelet-activating factor antagonist WEB 2086 in the treatment of asthma. *Am. J. Respir. Crit. Care Med.* 149:1142–1148. <https://doi.org/10.1164/ajrccm.149.5.8173754>
- Sutterwala, F.S., Y. Ogura, M. Szczepanik, M. Lara-Tejero, G.S. Lichtenberger, E.P. Grant, J. Bertin, A.J. Coyle, J.E. Galán, P.W. Askenase, and R.A. Flavell. 2006. Critical role for NALP3/CIAS1/Cryopyrin in innate and adaptive immunity through its regulation of caspase-1. *Immunity*. 24:317–327. <https://doi.org/10.1016/j.immuni.2006.02.004>
- Swanson, K.V., M. Deng, and J.P.Y. Ting. 2019. The NLRP3 inflammasome: molecular activation and regulation to therapeutics. *Nat. Rev. Immunol.* 19:477–489. <https://doi.org/10.1038/s41577-019-0165-0>
- Takeda, K., H. Tsutsui, T. Yoshimoto, O. Adachi, N. Yoshida, T. Kishimoto, H. Okamura, K. Nakanishi, and S. Akira. 1998. Defective NK cell activity and Th1 response in IL-18-deficient mice. *Immunity*. 8:383–390. [https://doi.org/10.1016/S1074-7613\(00\)80543-9](https://doi.org/10.1016/S1074-7613(00)80543-9)
- Tzeng, T.C., S. Schattgen, B. Monks, D. Wang, A. Cerny, E. Latz, K. Fitzgerald, and D.T. Golenbock. 2016. A Fluorescent Reporter Mouse for Inflammasome Assembly Demonstrates an Important Role for Cell-Bound and Free ASC Specks during In Vivo Infection. *Cell Reports*. 16:571–582. <https://doi.org/10.1016/j.celrep.2016.06.011>
- Van Anthony, M.V., S. Cuevas, X. Zheng, and P.A. Jose. 2016. Localization and signaling of GPCRs in lipid rafts. *Methods Cell Biol.* 132:3–23.
- Vincent, J.L., H. Spapen, J. Bakker, N.R. Webster, and L. Curtis. 2000. Phase II multicenter clinical study of the platelet-activating factor receptor antagonist BB-882 in the treatment of sepsis. *Crit. Care Med.* 28:638–642. <https://doi.org/10.1097/00003246-200003000-00006>
- Wen, H., D. Gris, Y. Lei, S. Jha, L. Zhang, M.T.-H. Huang, W.J. Brickey, and J.P.Y. Ting. 2011. Fatty acid-induced NLRP3-ASC inflammasome activation interferes with insulin signaling. *Nat. Immunol.* 12:408–415. <https://doi.org/10.1038/ni.2022>
- Wilson, J.E., A.S. Petrucelli, L. Chen, A.A. Koblansky, A.D. Truax, Y. Oyama, A.B. Rogers, W.J. Brickey, Y. Wang, M. Schneider, et al. 2015. Inflammasome-independent role of AIM2 in suppressing colon tumorigenesis via DNA-PK and Akt. *Nat. Med.* 21:906–913. <https://doi.org/10.1038/nm.3908>
- Xu, H., J. Yang, W. Gao, L. Li, P. Li, L. Zhang, Y.N. Gong, X. Peng, J.J. Xi, S. Chen, et al. 2014. Innate immune sensing of bacterial modifications of Rho GTPases by the Pyrin inflammasome. *Nature*. 513:237–241. <https://doi.org/10.1038/nature13449>
- Yan, Y., W. Jiang, L. Liu, X. Wang, C. Ding, Z. Tian, and R. Zhou. 2015. Dopamine controls systemic inflammation through inhibition of NLRP3

- inflammasome. *Cell*. 160:62–73. <https://doi.org/10.1016/j.cell.2014.11.047>
- Yang, J., Y. Zhao, J. Shi, and F. Shao. 2013. Human NAIP and mouse NAIP1 recognize bacterial type III secretion needle protein for inflammasome activation. *Proc. Natl. Acad. Sci. USA*. 110:14408–14413. <https://doi.org/10.1073/pnas.1306376110>
- Yost, C.C., A.S. Weyrich, and G.A. Zimmerman. 2010. The platelet activating factor (PAF) signaling cascade in systemic inflammatory responses. *Biochimie*. 92:692–697. <https://doi.org/10.1016/j.biochi.2010.02.011>
- Yu, J.R., and K.S. Leslie. 2011. Cryopyrin-associated periodic syndrome: an update on diagnosis and treatment response. *Curr. Allergy Asthma Rep.* 11:12–20. <https://doi.org/10.1007/s11882-010-0160-9>
- Zanoni, I., Y. Tan, M. Di Gioia, A. Broggi, J. Ruan, J. Shi, C.A. Donado, F. Shao, H. Wu, J.R. Springstead, and J.C. Kagan. 2016. An endogenous caspase-1 ligand elicits interleukin-1 release from living dendritic cells. *Science*. 352:1232–1236. <https://doi.org/10.1126/science.aaf3036>
- Zhao, C., D.D. Gillette, X. Li, Z. Zhang, and H. Wen. 2014. Nuclear factor E2-related factor-2 (Nrf2) is required for NLRP3 and AIM2 inflammasome activation. *J. Biol. Chem.* 289:17020–17029. <https://doi.org/10.1074/jbc.M114.563114>
- Zhao, Y., J. Yang, J. Shi, Y.N. Gong, Q. Lu, H. Xu, L. Liu, and F. Shao. 2011. The NLRP4 inflammasome receptors for bacterial flagellin and type III secretion apparatus. *Nature*. 477:596–600. <https://doi.org/10.1038/nature10510>
- Zhu, S., S. Ding, P. Wang, Z. Wei, W. Pan, N.W. Palm, Y. Yang, H. Yu, H.B. Li, G. Wang, et al. 2017. Nlrp9b inflammasome restricts rotavirus infection in intestinal epithelial cells. *Nature*. 546:667–670. <https://doi.org/10.1038/nature22967>